# Sources and Budgets for CO and $O_3$ in the Northeastern Pacific during the spring of 2001: Results from the PHOBEA-II Experiment

Lyatt Jaeglé,[1] Dan Jaffe,[2] Heather U. Price,[2, 3] Peter Weiss-Penzias,[2] Paul I. Palmer,[4] Mat J. Evans,[4] Daniel J. Jacob[4], and Isabelle Bey[5]

[1]Department of Atmospheric Sciences, BOX 351640, University of Washington, Seattle, Washington, 98195, USA. E-mail: jaegle@atmos.washington.edu. Phone: (206) 685-2679.

[2]Interdisciplinary Arts and Sciences, University of Washington Bothell, Bothell, Washington, 98011, USA. E-mails: djaffe@u.washington.edu, hprice@u.washington.edu, pweiss@bothell.washington.edu

[3]Also at Department of Chemistry, University of Washington, Seattle, Washington, 98195, USA.

[4]Division of Engineering and Applied Sciences and Department of Earth and Planetary Sciences, Harvard University, Cambridge, Massachusetts, 02138, USA. E-mails: pip@sol.harvard.edu, mje@sol.harvard.edu, djj@sol.harvard.edu

[5]Swiss Federal Institute of Technology (EPFL), DGR-LPAS, CH-1015 Lausanne, Switzerland. E-mail: isabelle.bey@epfl.ch

***Short title:*** NE PACIFIC CO AND $O_3$ BUDGETS

***Keywords***: Long-range transport; carbon monoxide; ozone; Pacific

***Index terms***: Troposphere – composition and chemistry (0322); Troposphere – constituent transport and chemistry (0368)

Submitted to the Journal of Geophysical Research – Atmospheres,
TRACE-P special issue, October 2002.

**Abstract.** Ground and airborne measurements of CO, ozone, and aerosols were obtained in the northeastern Pacific troposphere during March 9-May 31 2001 as part of the PHOBEA-II project (Photochemical Ozone Budget of the Eastern North Pacific Atmosphere). We use these observations together with the GEOS-CHEM global 3-D model of tropospheric chemistry to examine the origin of CO and ozone in the NE Pacific troposphere. The GEOS-CHEM model successfully reproduces the observed CO levels, their temporal variability, and vertical gradients, implying a good understanding of the sources, transport and chemistry of CO in the NE Pacific. For ozone the model reproduces the airborne profiles well, but systematically underestimates mean surface observations by 11 ppbv. We find a pervasive influence of Asian as well as European anthropogenic sources on the levels of CO in the NE Pacific troposphere. In the 0-6 km column over our surface site, Asian and European emissions account for 33% (43 ppbv) and 16% (25 ppbv) of CO, respectively. Because of the shorter lifetime of ozone relative to CO, Asian and European emissions are responsible for smaller fractions of the 0-6 km ozone column, 12% and 5%, respectively, based on direct transport of ozone produced in the lower troposphere over these regions. The full influence of Asian emissions (including secondary ozone production by export of its precursors) approaches 16% of ozone. The budget of odd-oxygen in the NE Pacific below 6 km is characterized by net loss: photochemical loss and deposition are partly counterbalanced by westerly advection and photochemical production. The model successfully reproduces three cases of rapid intercontinental transport events observed during the spring 2001 campaign: one at the surface and two in the free troposphere. While all three events were characterized by large CO enhancements (by 20-40 ppbv), only one case showed significant ozone enhancement (by 20 ppbv), induced by long-range transport of Asian pollution at high latitudes together with a stratospheric ozone contribution.

## 1. Introduction

Ozone and carbon monoxide play key roles in the troposphere. Tropospheric ozone controls the oxidizing power of the atmosphere. At the surface, it is a major pollutant, harmful to human health and vegetation. In the middle and upper troposphere, ozone is an important greenhouse gas. Ozone is transported to the troposphere from the stratosphere, and is also produced in the troposphere by the oxidation of CO and nonmethane hydrocarbons (NMHC) in the presence of nitrogen oxides ($NO_x$=NO+$NO_2$) and hydrogen oxides ($HO_x$=HO+$HO_2$) [e.g., *WMO*, 1999].

Carbon monoxide provides the primary OH sink in much of the troposphere. In addition CO is a useful tracer of anthropogenic activities. The major sources of CO are fossil fuel combustion, biomass burning, biofuel burning, oxidation of atmospheric $CH_4$ and of NMHCs [*Logan et al*., 1981]. The lifetime of CO is in the range of weeks to months, while ozone has a shorter lifetime, ranging from days to weeks, depending upon the environment.

Observations from the late 19$^{th}$ and early 20$^{th}$ century combined with models suggest that northern hemisphere tropospheric ozone concentrations have increased by 25-50% since preindustrial times due to increasing anthropogenic $NO_x$, CO, and NMHC emissions from fossil fuel combustion and biomass burning [*Prather and Ehhalt*, 2001, and references therein]. East Asia, in particular, is a region experiencing rising emissions due to rapid economic growth over the last few decades [*Akimoto and Narita*, 1994; *Elliott et al*., 1997; *van Aardenne et al*., 1999; *Streets and Waldhoff*, 2000]. As a result, ozone in the boundary layer and lower troposphere of East Asia has been increasing by about 2% per year [*Logan*, 1994; *Lee et al*., 1998]. Continued increases in $NO_x$ and NMHC emissions, especially in developing regions of the world, may

cause tropospheric $O_3$ to increase more dramatically through the 21st century [*Prather and Ehhalt*, 2001].

Observations have shown that Asian emissions of gases and aerosols can be transported to North America in 6-8 days, under certain meteorological conditions [*Andreae et al*., 1988; *Kritz et al*., 1990; *Parrish et al*., 1992; *Jaffe et al*., 1999, 2001, 2002; *Husar et al*., 2001; *McKendry et al*., 2001; *Kotchenruther et al*., 2001a; *Price et al*., 2002; *Thulasiraman et al*., 2002]. Enhanced mixing ratios of CO, Peroxyacetyl nitrate (PAN), NMHCs, industrial and mineral aerosols, radon, and sulfate have been identified in these airmasses coming from East Asia. However not all of these airmasses with clear anthropogenic signatures are characterized by ozone enhancements [*Jaffe et al*., 2002], suggesting loss of ozone during transport over oceans or reduced photochemical production over emission areas. Identification of ozone enhancements due to transport of Asian emissions is further complicated by the possible mixing of anthropogenic emissions with stratospheric ozone [*Carmichael et al*., 1998].

Based on chemical transport model (CTM) calculations, current emissions from Europe and Asia contribute on average 4-7 ppbv $O_3$ at the surface in North America [*Berntsen et al*., 1999; *Jacob et al*., 1999; *Yienger et al*., 2000; *Wild and Akimoto*, 2001; *Fiore et al*., 2002]. A future doubling of Asian emissions might increase surface ozone by another 4 ppbv over Western North America [*Bernsten et al*., 1999]. Such an increase would offset the benefits from domestic reductions in anthropogenic emissions in the U.S. [*Jacob et al*., 1999]. However, these estimates remain highly uncertain, and current understanding of intercontinental transport of Asian effluents and their effects on the global troposphere are limited by the lack of observations constraining the CTM calculations of Asian sources, transport and chemical transformation.

During the spring of 2001 the TRACE-P (Transport and Chemical Evolution over the Pacific) [*Jacob et al*., this issue] and ACE-Asia (Aerosol Characterization Experiment-Asia) [*Huebert et al*., 2002] experiments were both operating in the western North Pacific region, where they sampled the gas and aerosol composition of the Asian outflow. Simultaneously, we made ground and airborne observations in the northeastern Pacific as part of the PHOBEA-II project (Photochemical Ozone Budget of the Eastern North Pacific Atmosphere). The main goal of PHOBEA project is to understand the impact of upstream anthropogenic emissions on the NE Pacific troposphere [*Jaffe et al*., 2001; *Kotchenruther et al*., 2001a]. During these three missions, several CTMs [*Kiley et al*., this issue] were used for flight planning to optimize the value of observations in constraining and evaluating CTM simulations of Asian sources, outflow and chemical evolution [*Jacob et al*., this issue].

In this paper we utilize the PHOBEA-II ground and airborne observations in the Northeastern Pacific during the spring of 2001, along with the GEOS-CHEM global model of tropospheric chemistry [*Bey et al*., 2001a] to understand the sources of atmospheric CO and $O_3$ in the northeastern (NE) Pacific. *Price et al.* [2002, this issue], give a detailed description of the results from the airborne component of PHOBEA-II. In parallel papers in this issue, the GEOS-CHEM model is used to interpret the TRACE-P observations in the western Pacific [*Liu et al*., this issue; *Palmer et al*., this issue; *Bey et al*., this issue]. Our focus in this paper is to evaluate the current effects of Asian and European outflow in the NE Pacific. In particular we wish to address the following questions: How well can global models reproduce the observed mixing ratios and variability of CO and $O_3$ in the NE Pacific? What are the sources and budgets for CO and $O_3$ in the NE Pacific? Can global model simulations quantitatively capture intercontinental transport events arriving in the NE Pacific?

## 2. Observations and Model

The PHOBEA-II mission combined surface observations at the Cheeka Peak Observatory (CPO, 48.3˚N, 124.6˚W, 480 m) on the western tip of Washington State and airborne profiles to 6 km altitude in the area immediately off the coast from CPO. During the first phase of the PHOBEA experiment, we used this site for observations during March-April 1997 and March-April 1998 [*Jaffe et al*., 2001], and conducted airborne measurements off the coast in the spring of 1999 [*Kotchenruther et al*., 2001a].

### *2.1. Ground-based observations*

For this work, we began ground-based measurements of CO, $O_3$, PM10 and PM2.5 at CPO on March 9, 2001. The experimental methods for CO and $O_3$ are identical to those given in *Jaffe et al*., [2001]. Briefly, CO was measured by a commercial gas filter correlation infra-red instrument (Advanced Pollution Instruments model 300) modified for higher sensitivity [*Jaffe et al*., 1998]. Calibration occurred once per day with a working standard referenced to a NIST standard reference material. An instrument zero is performed every 20 minutes by routing the airstream through a heated catalyst that oxidizes CO to $CO_2$. Ozone was measured using a standard UV absorption instrument (Dasibi AH1008) with temperature and pressure compensation. Calibration of the ozone instrument was performed using a standard $O_3$ calibrator immediately prior to the campaign and zero checks were performed daily.

### *2.2. Vertical profiles*

For the vertical profiles we used a twin-engine Beechcraft Duchess aircraft with a ceiling of 6 km altitude. Profiles were conducted on 12 days between March 29 and May 6, 2001. The Duchess aircraft can carry the pilot plus one passenger and approximately 240 kg of instrumentation. The plane was equipped to make in-situ measurements of $O_3$ by UV absorption

(2B Technologies) and aerosol scatter at 3 wavelengths (700, 550, 450 nm; TSI model 3563), and collected whole air samples in stainless steel canisters for measurements of CO (by gas chromatography with a reduction gas analyzer detector) and NMHCs (by gas chromatography with flame ionization detector). The new lightweight $O_3$ instrument [*Bognar and Birks*, 2000] was extensively tested against a standard UV instrument as well as against an ECC ozonesonde [*Snow et al*., 2002]. The lighter $O_3$ instrument yielded accurate measurements when compared with the other two methods, but it had lower precision. *Price et al.* [2002, this issue] give more details on the instrumentation, calibration procedures and flight patterns for the Duchess vertical profiles.

### *2.3. GEOS-CHEM model*

Global simulations of $O_3$-$NO_x$-NMHC chemistry are conducted with the GEOS-CHEM global 3-D model of tropospheric chemistry [*Bey et al*., 2001a] driven by GEOS DAO (Data Assimilation Office) assimilated meteorological data [*Schubert et al*., 1993]. The simulations presented here use GEOS-CHEM version 4.32 (http://www.as.harvard.edu/chemistry/trop/geos/) and two years (2000-2001) of GEOS assimilated meteorological observations with a horizontal resolution of 2° latitude by 2.5° longitude and 46 vertical layers. Meteorological inputs are available with a 3- to 6-hour time resolution depending on the variable. The simulations are initialized on February 1, 2001 after a one-year spin-up with a 4° x 5° horizontal resolution to speed up the calculations.

The tropospheric $O_3$ simulation includes a complete description of $O_3$-$NO_x$-NMHC chemistry (24 tracers and 120 species) [ *Bey et al.*, 2001a]. Recent updates to the GEOS-CHEM model are described in *Palmer et al.* [this issue], and include in particular a treatment of the heterogeneous and photochemical effects of aerosols [*Martin et al*., 2002a]. Fossil fuel and

biofuel emission inventories are from *Duncan et al.* [2002a] and *Yevich et al.* [2002], and are scaled to the year 1998. We use the seasonally varying climatological biomass burning emissions of *Duncan et al*. [2002b]. Analysis of satellite observations show that Asian biomass burning emissions during spring 2001 were close to average [*Heald et al*., this issue], justifying the use of a climatological average. For CO, our anthropogenic emissions for Asia (10°S-60°N, 60°-150°E) are 257 Tg $yr^{-1}$ (fossil fuel: 160 Tg $yr^{-1}$; biofuel: 97 Tg $yr^{-1}$), with an additional 119 Tg $yr^{-1}$ from biomass burning.

The GEOS-CHEM tropospheric chemistry model has been extensively evaluated and used to study ozone and its precursors over different regions of the globe [e.g., *Bey et al*., 2001ab; *Liu et al*., 2002; *Fiore et al*., 2002; *Palmer et al*., 2001; *Li et al*., 2002ab; *Martin et al*., 2002b]. In particular, the GEOS-CHEM model reproduces well the observed latitudinal and vertical composition of the Asian chemical outflow over the western Pacific, as well as its episodic export [*Bey et al*., 2001b; *Liu et al*., 2002; *Liu et al*., this issue; *Palmer et al.*, this issue].

To investigate the origin of CO and ozone in the model we conducted two sensitivity simulations based on the full chemistry ozone simulation: (1) a tagged CO simulation resolving source regions using archived monthly averaged OH concentrations; (2) a tagged ozone run using archived daily rates of odd oxygen ($O_x = O_3 + NO_2 + 2\times NO_3 + HNO_3 + PAN + HNO_4 + 3\times N_2O_5$) production rates and loss frequencies. For the tagged CO simulation [*Bey et al*., 2001b; *Li et al.,* 2002a], we focus on four anthropogenic tracers, "North American FF CO", "Asian FF CO", "Asian BB CO" and "European FF CO" (specific geographical regions are defined in Table 1). Each of the "FF" tracers combines contributions from fossil fuel and biofuel sources, while the Asian "BB" tracer refers to biomass burning sources. For all the results presented here the "Asian CO" tracer will refer to the sum of FF and BB Asian CO tracers. Loss of CO by

reaction with OH and production of CO by oxidation of methane and NMHCs are calculated using monthly averaged OH concentrations from the full chemistry simulation. The tagged ozone simulation [*Li et al*., 2002a; *Liu et al*., 2002] transports eight $O_x$ tracers from different regions. Results will be presented for ozone originating in the stratosphere, upper troposphere (400 hPa-tropopause), middle troposphere (700-400 hPa) and lower troposphere (700 hPa-surface). The lower troposphere is further subdivided into three separate continental tracers (Asian, European and North American, see Table 1 for geographical regions) and one tracer over the Pacific Ocean. We will refer to the tagged $O_x$ tracers as "tagged ozone" tracers as ozone generally represents more than 95% of $O_x$.

The tagged ozone simulation gives information on the direct export of ozone produced in the lower troposphere over the continent of origin: "tagged Asian ozone" represents the ozone produced from ozone precursors (natural and anthropogenic) within the lower troposphere above Asia. Evaluating secondary production of ozone resulting from free tropospheric transport of ozone precursors from Asian is less straightforward. Our approach is to conduct a simulation with Asian anthropogenic sources turned off. The difference (*delta* $O_3$ = standard simulation – simulation without Asian sources) should reflect the combined effects of direct transport and secondary production. One caveat is that the non-linearity of ozone production results in an overestimate of ozone production from natural sources close to the continent of origin, and thus an underestimate of Asian contribution. We will thus estimate a lower limit of the contribution from exported precursors by comparing "delta $O_3$" to the "tagged Asian ozone" tracer.

**3. Use of global model forecasting to identify flight days**

Vertical profiles were made on 12 days between March 29 and May 6, 2001. Consistent with the goals of the PHOBEA experiment, we targeted days when long-range transport from

sources on the Eurasian continent seemed likely. We also sought to sample clean marine airmasses. However, we endeavored to avoid days affected by recent emissions from the west coast of North America. A number of tools were used to identify the flight days. This includes the GEOS-CHEM forecast results [*Bey et al*., this issue] driven by meteorological GEOS-3 forecasts from NASA Goddard (http://polar.gsfc.nasa.gov/operations/terra.php). We also used local meteorological data, results from the University of Washington's high resolution MM5 simulations, satellite infrared and visible imagery, the TOMS aerosol index and forecast trajectories using NOAA's Hybrid Single-Particle Lagrangian Integrated Trajectory (HYSPLIT) model [*Draxler and Hess*, 1997].

As an example of the use of the model forecasts, Figure 1 shows the GEOS-CHEM CO forecast for April 13, 2001 at 6 GMT. This 3-day 'look-ahead' forecast was initialized 0 GMT on April 10. On April 13, an airmass with a high mixing ratio of CO from Asia was predicted to be near the coast of Washington state. We conducted a vertical profile on April 14, 2001 between 1 and 2 GMT and indeed found significantly enhanced CO, aerosols and NMHCs at 4-6 km altitude [*Price et al*., this issue]. In fact the CO and NMHC mixing ratios and the aerosol scattering coefficient in this airmass were the largest we observed during the spring of 2001. This airmass appears to have started as a large dust storm that originated in central Asia in early April and left the Asian continent on April 8 after picking up substantial amounts of anthropogenic emissions as it crossed East Asia. The dust storm was detected by the TOMS satellite Aerosol Index (AI) product and the SeaWIFS sensors as it moved across the Pacific [*Price et al*., this issue; *Thulasiraman et al*., 2002; *Huebert et al*., 2002].

We need to assess whether our sampling strategy resulted in a dataset representative of all types of airmasses and chemical conditions characteristic of springtime NE Pacific troposphere.

We thus compare CO column densities up to 6 km above CPO, both for the observations and the GEOS-CHEM model, to minimize effects from times when the model identifies an incorrect altitude for a pollution layer (Figure 2). Here and in the rest of this paper we exclusively use the GEOS-CHEM post-mission model results driven by assimilated meteorology. For the days when measurements were made, the average 0-6 km CO column was $1.53 \cdot 10^{18}$ molecules/cm$^2$ from the data and $1.46 \cdot 10^{18}$ molecules/cm$^2$ from the GEOS-CHEM model, showing good agreement. The modeled column for the March 29-May 5 period is $1.45 \cdot 10^{18}$ molecules/cm$^2$. The similarity of the modeled column for all dates and the column for just the flight days indicates that the flight days are a good representation of the entire time period, at least for CO. Figure 2 also illustrates the effects of certain flight day decisions. For example the flights conducted on April 1, 5, and 8 were targeted to test the ability of the model to reproduce variations in transport and the resulting effects on atmospheric composition. On these dates the model forecasts indicated alternating influences going from high CO to aged marine air with lower CO and back to high CO. This pattern was confirmed by the observations.

## 4. Comparison of model and observations

**Carbon monoxide**. Figure 3 shows the hourly-averaged observed CO mixing ratios at the CPO ground-site along with the hourly GEOS-CHEM modeled values between March 9 and May 31, 2001. The model generally captures the observed levels, the slow decline of CO throughout April and May (resulting from increasing levels of OH radical), as well as the timing and magnitude of periods with enhanced and low concentrations. The events with high levels of CO (>200 ppbv) correspond to extended periods of easterly winds bringing air recently influenced by North American emissions (March 20; April 15; May 20; May 31). These

conditions generally occur when a surface high pressure system moves inland over the Pacific Northwest, resulting in low-level off-shore flow. Two notable exceptions to the good agreement are April 4 (model overpredicts observations by 40 ppbv) and May 13-16 (model underpredicts observations by 50 ppbv), which are characterized the poor performance of the coarse 2°×2.5° resolution wind fields in capturing sharp gradients in meteorological conditions near CPO.

Overall, there is excellent agreement between modeled CO (148±19 ppbv) and observed CO (151±17 ppbv) for the time period of observations (Figure 5a). The correlation coefficient indicates that the model captures 53% of the day-to-day variability in CO. The spring 2001 CO observations are similar to 1997 observations (159 ppbv) but much lower than the observations in 1998 (177 ppbv) at CPO. *Jaffe et al.* [1999] attribute the higher values in 1998 to unusually high biomass burning emissions in Indonesia and Siberia.

Figure 4 shows a comparison of observed and modeled CO mixing ratios as seen in the vertical profiles. One difficulty in this comparison is the short timescale (~1 hour) and small spatial extent of the Duchess flights relative to the longer timescale on which wind fields are updated (6 hours) and the coarse horizontal resolution of the model. Given the variability in hourly CO levels (Figures 2 and 3), a small displacement in time might lead to large discrepancies between modeled and observed profiles. To overcome this difficulty, we plot the profile sampled at the time and location of the observations, and four other profiles displaced in time by ±6 hours and ±12 hours. For most of the flights, there is little variability in the modeled profiles, reflecting the spatial uniformity of the modeled CO fields. However, in a few cases, such as March 31, April 5, and May 6 there are larger differences. The first two days correspond to periods of easterly low levels winds bringing increasing amounts of North American CO to

the region, while the May 6 case shows the arrival of an Asian CO plume (further discussion on the May 6 observations is in section 7).

For the vertical profiles, the mean measured CO mixing ratio was 139±20 ppbv, compared to a mean modeled value for the ensemble of flights of 136±16 ppbv, showing very good agreement (Figure 5b). The elevated correlation coefficient ($r^2$ = 0.54) reflects the model's ability in capturing observed variability. The 2001 airborne profiles of CO show no statistically significant difference relative to the 1999 observations [*Price et al.*, this issue].

The excellent agreement between model and observations for CO implies that the GEOS-CHEM model is accurately simulating the emission sources, transport, and CO chemistry. In contrast, comparisons between CO observations obtained in the Eastern Pacific during TRACE-P and chemical transport models show a significant negative bias of the models [*Kiley et al*., this issue]. All the models in the intercomparison used the detailed CO fossil fuel and biofuel emission inventory developed by *Streets et al.* [this issue] for Asia in 2000 (212 Tg $yr^{-1}$), which is 20% lower than our emission inventory (257 Tg $yr^{-1}$). An inverse modeling analysis [*Palmer et al.*, this issue] suggests that an increase in anthropogenic emissions over China close to the levels used in our study, largely eliminates the model bias. *Streets et al.* [this issue] attribute the underpredition of Chinese emissions in their study to an under-reporting of domestic coal use in central China.

**Ozone**. Figure 6 shows a comparison of measured $O_3$ at CPO, along with the modeled values and Figure 7 shows a similar comparison for the vertical profiles. At the ground, the model systematically underestimates the observations by 11 ppbv (observations: 47±5 ppbv; model: 36±4 ppbv), while aloft the model reproduces the observed mean well (observations: 45±9 ppbv; model: 46±7 ppbv) (Figure 5c and 5d). The weak correlation coefficient between

model and observations ($r^2$<0.2) reflects the small variability of observed ozone and the overestimate of North American influence on ozone (section 6). Comparison of the GEOS-CHEM model to ozonesonde observations at Trinidad Head, California during spring 2001 (not shown) also reveals a systematic underestimate, but with a smaller bias of 2-5 ppbv. In addition, the model systematically underpredicts observed ozone levels in the western Pacific during TRACE-P by 10 ppbv [*M.J. Evans*, personal communication]. Reasons for this bias could include problems with the Asian $NO_x$ emissions, or an overestimate of stratospheric ozone columns (which would decrease photolysis rates) [*M.J. Evans*, personal communication].

The springtime observations of ozone obtained at CPO in 2001 are very similar to mean observations from the 1997 and 1998 (1997: 43 ppbv, 1998: 45 ppbv). While the airborne ozone profiles in 2001 are on average 11 ppbv lower than the profiles obtained in 1999 [*Kotchenruther et al*., 2001a]. *Price et al.* [this issue], attribute the greater levels of ozone in 1999 to enhanced stratosphere-troposphere exchange and/or biomass burning.

**5. Pathways for long-range transport of CO and ozone to the North Eastern Pacific**

The distribution of average (0-6 km) CO and ozone mixing ratios for the North American, Asian and European tagged tracers are shown in Figure 8, along with their respective horizontal fluxes. The concentrations and fluxes are averaged over the two and a half month time period of the 2001 PHOBEA-II campaign. Figure 9 shows the vertical distribution of concentrations and westerly fluxes of these tracers for a latitudinal cross-section at 125°W, along the west coast of North America.

**North American influence**

Over the Eastern United States, frontal lifting of North American boundary layer air towards the Atlantic is the dominant export pathway of pollution [*Stohl and Trikl, 1999; Stohl*, 2001*; Cooper et al.*, 2002; *Li et al*., 2002a]. A small fraction of North American pollution can also be exported to the Pacific through three pathways: (1) episodic easterly low level flow north of 40°N (discussed in section 4); (2) northeasterly flow on the southern branch of the Pacific high south of 30°N; and, (3) circumpolar circulation reaching the Pacific. These pathways result in 10-20 ppbv CO over the NE Pacific (Figure 8a). Westerly circumpolar transport through pathway (3) extends throughout the free troposphere, resulting in $1\text{-}2\cdot10^{-10}$ moles CO $s^{-1}$ $cm^{-2}$ between 2 and 10 km, while easterly transport via (1) and (2) occurs in the lower troposphere south of 30°N and north of 40°N (Figure 9a).

Springtime ozone production in North America is restricted to low latitudes in the South-East United States. With its shorter lifetime due to photochemistry and surface deposition, North American ozone is exported less efficiently relative to CO, contributing only 2-4 ppbv of ozone over the northern Pacific (Figure 8d). The largest influence is found off Baja California with up to 20 ppbv coming from anthropogenic American emissions (via pathway 2). The vertical distribution of North American ozone fluxes at 125°W (Figure 9d) shows that westerly transport of North American ozone results in a $0.5\text{-}1\cdot10^{-10}$ moles $O_3$ $s^{-1}$ $cm^{-2}$ flux between 2 and 12 km (pathway 3), while stronger easterly fluxes (up to $2.5\cdot10^{-10}$ moles $O_3$ $s^{-1}$ $cm^{-2}$) occurs in the lower troposphere for latitudes south of 30°N (pathway 2), fueled by large rates of ozone production. Some of the ozone and CO transported through pathway (2) can influence the composition of the Northern Tropics [*Staudt et al*., 2001].

**Asian Influence**

*Liu et al.* [this issue] and *Carmichael et al*. [this issue] show that the major processes driving export of Asian anthropogenic pollution to the Pacific during spring 2001 are frontal lifting in warm conveyor belts ahead of cold fronts and boundary layer transport behind the cold fronts. In addition, convection over South East Asia is important for driving the export of biomass burning emissions south of 30ºN. Once over the Pacific, rapid westerly winds throughout the troposphere can transport Asian anthropogenic and biomass burning effluents across the Pacific [*Jaffe et al*., 1999; *Yienger et al*., 2000].

Asian sources account for 40-50 ppbv of CO in the NE Pacific troposphere (Figure 8b), roughly one third of the total CO (Table 1), consistent with previous analyses [*Berntsen et al*., 1999; *Yienger et al*., 2000; *Staudt et al*., 2000]. Most of this Asian CO originates from fossil fuel combustion, with only 5-10 ppbv coming from biomass burning emissions, based on our climatological biomass burning emission inventory. Asian sources affect a large region of the NE Pacific, from the surface to 12 km altitude between 30 and 60°N (Figure 9b). This Asian influence shows a maximum at 4-10 km where warm conveyor belts deposit most of the transported CO [*Yienger et al*., 2000; *Stohl*, 2001; *Liu et al*., this issue]. At these altitudes the westerly fluxes reaches $10\text{-}15 \cdot 10^{-10}$ moles CO $s^{-1}$ $cm^{-2}$ (Figure 9b), but substantial fluxes ($>5 \cdot 10^{-10}$ moles CO $s^{-1}$ $cm^{-2}$) are also reaching lower altitudes, illustrating the importance of boundary layer transport of Asian CO across the Pacific.

Direct transport of surface ozone produced over Asia results in 4-6 ppbv of ozone in the NE Pacific, roughly 10% of total ozone (Figure 8e). Figure 9e shows a maximum Asian ozone

contribution of 6-8 ppbv between 2 and 10 km altitude, induced by faster westerly transport and a longer lifetime for ozone.

The Asian tagged ozone represents transport of ozone produced within the Asian lower troposphere, but does not account for secondary ozone production via export of $NO_x$ and PAN from Asia. The difference between our standard full chemistry simulation and a simulation without Asian anthropogenic sources simulation (*delta $O_3$*) is a lower estimate of the combined direct transport and secondary ozone production from Asia (see section 2.3). By comparing Figure 10a and Figure 8e, we find that the influence of secondary ozone production increases ozone by 2-4 ppbv on average in the NE Pacific for the 0-6 km column, and is particularly significant in the areas influenced by the subsidence in the Pacific High pressure system. At the surface, there is only a 10-20% increase in ozone, reflecting the minor role of secondary production at low altitudes (compare Figure 10b to Figure 9e). However, in the upper troposphere over the eastern Pacific secondary production results in a doubling of the Asian impact on ozone between 10 and 30°N. At these low latitudes, convection is the dominant export pathway from Asia [*Liu et al*., this issue], and thus rapid lifting of Asian $NO_x$ followed by efficient ozone production during transport becomes a significant source of ozone.

**European influence**

Export of European pollution is generally confined to the lower troposphere below 3 km altitude [*Staudt et al*., 2001], as a result of the high latitudes of emissions and the relative infrequency of cyclogenesis to efficiently vent the boundary layer [*Stohl*, 2001]. The main pathway for export of European pollution is northward to the Arctic [e.g., *Raatz*, 1989]. However, under the influence of the Siberian anticyclone, a fraction of European emissions is transported towards Asia [*Newell and Evans*, 2001; *Bey et al*., 2001b], where it accounts for 30-

50 ppbv CO and 4-6 ppbv of ozone (Figures 8c and 8f). After reaching the East coast of Asia, the pollution can then be exported to the Pacific in post-frontal boundary layer outflow where it mixes with Asian pollution [*Liu et al*., this issue], and is carried in the storm track across the Pacific, mostly remaining at low altitudes and high latitudes (Figures 9c and 9f). This type of low-level transport is not efficient for ozone, which has a short lifetime in the lower troposphere; however, European CO can reach the United States. Overall the European influence results in 20-30 ppbv CO and 2-4 ppbv ozone in the NE Pacific (Figures 8c and 8f).

**6. Origin of CO and ozone at CPO**

Springtime CO concentrations at the CPO ground site are dominated by anthropogenic sources from Asia (43 ppbv), with significant contributions from North American (25 ppbv) and European (25 ppbv) sources (Figure 3, Table 1). The Asian contribution is mostly from fossil fuel and biofuel sources, and only a small amount comes from biomass burning (7 ppbv). Most of the remaining CO comes from oxidation of methane and biogenic NMHCs. At the surface, 77% of the variability in the modeled CO is controlled by the variability in the North American source. Variability in Asian and European source contributions explain an additional 20% of the variability. Enhancements in Asian and European contributions often coincide (Figure 3), reflecting their mixing in post-frontal boundary layer outflow over the East Asian coast. With increasing altitude, the relative contributions from European and North American sources decrease while the Asian contribution increases (Figure 4).

In contrast to CO, the Asian and European contributions to ozone levels are much smaller (Figures 6 and 7). At CPO, based on our tagged-ozone simulation, we find that 4.2 ppbv (11%) originate from production in the Asian lower troposphere (with an additional 1.5 ppbv coming

from secondary production), while 2.2 ppbv (6%) come from Europe, and 7 ppbv (18%) from North America, as summarized in Table 2. The remaining contributions are mostly from chemical production over the Pacific, middle and upper troposphere, and stratosphere. The North American contribution explains 27% of the modeled ozone variability, while the Asian and European contributions together explain another 25% of ozone variability. However, the model appears to overestimate the North American influence on ozone at CPO: increases in total ozone associated with the many high North American $O_3$ events in Figure 6 (coinciding with CO enhancements in Figure 3), are not present in the observations. Measurements at CPO during spring 1997 and 1998 [*Jaffe et al.*, 1999] often showed high concentrations of $NO_x$, PAN and CO associated with ozone titration during easterly flow from the nearby Seattle/Vancouver/Portland urban areas. With its 2°x2.5° horizontal resolution, the model dilutes $NO_x$ emissions from nearby regions resulting in ozone production in the model. This overestimate of North American production explains the poor correlation coefficient between model and observations (section 4).

How representative of the NE Pacific are measurements made at the ground and above CPO? To answer this question we compare modeled tropospheric columns (up to 6 km) averaged over the NE Pacific (defined as 165-125ºW; 35-65ºN) to the columns at CPO (Tables 1 and 2). For CO the columns are almost identical ($16.6 \cdot 10^{17}$ molecules/cm$^2$ in the NE Pacific, and $16.8 \cdot 10^{17}$ molecules/cm$^2$ above CPO), reflecting the fact that the 0-6 km column near CPO is indeed representative of the NE Pacific. The only difference comes from a slightly larger influence of North American contribution at the surface. For tagged-ozone, the North American influence dominates even more at CPO relative to the average NE Pacific columns (Table 2), but is likely to be due to the model's overestimate of North American influence noted above.

Table 3 presents the terms contributing to the modeled $O_x$ budget in the NE Pacific during PHOBEA-II. We have subdivided the budget into three altitude regions: below 3 km altitude there is a net loss of $O_x$; between 3 and 6 km altitude the $O_x$ budget is nearly balanced; between 6 and 12 km altitude there is a net production of $O_x$. In the lower part of the troposphere (< 2 km), the $O_x$ sources are controlled by advection from the west, descent from higher altitudes, and photochemical production. These sources are more than balanced by sinks in the form of advection out of the region through the East, North and South, deposition, and photochemical loss. Subsidence in the Pacific High pressure system appears as an important mechanism for supplying $O_x$ to the NE Pacific lower troposphere. In the middle and upper troposphere the dominant $O_x$ source is westerly advection, which increases with increasing altitude. Below 6 km there is net photochemical loss of ozone in NE Pacific region, consistent with the photochemical box model analysis of *Kotchenruther et al*. [2001b].

## 7. Case studies of trans-Pacific transport of pollutants

The episodic nature of trans-Pacific transport [e.g., *Jaffe et al*., 1999; *Yienger et al*., 2000; *Hess et al*., 2000] can be clearly seen at CPO in Figures 3 and 6, as well as in Figure 11, which shows the time-height dependence of Asian and European contributions to CO above CPO. Strong long-range transport episodes with Asian CO> 60 ppbv occur on twelve separate times (see Figure 11) and are seen much more frequently in the middle and upper troposphere compared to the lower troposphere, where only one such episode is predicted by the model, on March 11 2001. This lower tropospheric long-range transport episode resulted in an increase in CO observed at CPO, lending confidence to the model calculations (arrow on Figure 3). Two other Asian long-range transport episodes with smaller CO enhancements can also be noted in

the observations and the model on Figures 3 and 11: April 6-8 and April 28-29 2001. *Jaffe et al.* [2002] identified three episodes of long-range transport in the spring 2001 PHOBEA-II aircraft profiles for March 29, April 14, and May 6. Significant gas and aerosol layers were observed on all three flights and back trajectories suggest Asian industrial sources sometimes accompanied by mineral dust. The GEOS-CHEM model misses the March 29 event. However, the model does capture the April 14 and May 6 cases (Figures 4 and 7), and attributes the CO enhancements to transport of Asian pollution, consistent with the interpretation of *Jaffe et al.* [2002]. We now focus on a case-by-case analysis of these three long-range transport events which were observed in the NE Pacific and captured by the model: March 11, April 14, and May 6 2001.

**7.1. March 11 2001.**

This event is unique in two respects: the large contribution from Asian sources, exceeding 60 ppbv at the ground, and the vertical extent of the enhancements, which occurred throughout the troposphere, reaching a maximum of 115 ppbv Asian CO at 6 km altitude (Figure 11). Figure 2 shows a 30% increase in modeled column CO below 6 km altitude. NOAA HYSPLIT back trajectory calculations (not shown) indicate low-level transport from Asia with a transit time of 7 days at the surface, and a more rapid transit in the middle troposphere, confirming the GEOS-CHEM results. The observations exhibited enhanced CO for a 24-hour time period (~30 ppbv enhancement relative to mean spring levels), but no enhancements in ozone or aerosols. The model captures the timing of this event remarkably well, but somewhat underestimates the increase in CO (Figure 3). The model also predicts an increase in Asian ozone to 8 ppbv (Figure 6). These are the largest levels of Asian ozone calculated at CPO for spring 2001, but the

resulting small increase (~5 ppbv) in ozone on top of the background levels is difficult to identify in the total modeled ozone levels, consistent with lack of enhancement in the $O_3$ observations.

This long-range transport event has its origin in an intrusion of cold mid-latitude air deep into the South China Sea in early March 2001. This 'cold-surge' was associated with a surface cold front extending to northern Japan. Using the GEOS-CHEM model, *Liu et al.* [this issue] find that lifting of pollution ahead of the cold front over South China lead to the highest eastward flux of CO in the lower free troposphere over the western Pacific in spring 2001.

Figure 12, presenting average mixing ratios of Asian CO between 0 and 6 km as well as horizontal fluxes and sea level pressure maps, illustrates the sequence of events between March 4 and March 11 2001. The low pressure system at 42°N, 150°E forced Asian pollution outflow over the Pacific to the northeast, with maximum horizontal fluxes between 25° and 40°N on March 4. Over the next few days the cyclone traveled on a northeast trajectory in the Pacific storm track. By March 8, the Asian CO was located in the lower troposphere behind the cold front, as well as ahead of the cold front in the warm conveyor belt, where it ascended to the middle troposphere with a southerly flow. On March 7 and 9, the TRACE-P DC-8 aircraft flew out of Hong Kong across the cold front. Lifting of Asian CO ahead of the cold front between 4 and 8 km altitude was apparent in both observations and in model simulations [*Liu et al*., this issue; *Carmichael et al.*, this issue]. Strong subsidence capped the high levels of CO observed in the boundary-layer outflow behind the cold front.

Strong wind speeds throughout the troposphere allowed rapid transport of this Asian pollution across the Pacific. The upper tropospheric leading edge of the Asian CO tracer reached the North American coast on March 10 at 12 GMT (Figure 11). It was followed one day later by the lower tropospheric CO, channeled between the low pressure system over the Gulf of Alaska

and the Pacific high (Figure 12). By that time some of the upper tropospheric Asian CO started subsiding on the east side of the Pacific anticyclone off the Oregon and California coasts.

**7.2. April 14 2001**

The April 14 case was discussed by *Price et al.* [this issue] and *Jaffe et al.* [2002], and appears to have started as a large dust storm induced by a low-pressure system passing over the Gobi desert on April 6 2001 [*Gong et al*., 2002]. Over the next few days the system intensified and moved towards northeast Asia, passing over areas with high anthropogenic emissions. It then rapidly crossed the Pacific and, on April 13, the leading edge of the pollution plume reached the Washington and Oregon coasts between 2 and 6 km altitude (Figures 1 and 11).

On April 14 the observed CO was significantly enhanced between 4 and 6 km altitude, reaching 173 ppbv, but ozone showed little to no enhancement (Figure 7). The GEOS-CHEM model predicts a somewhat smaller CO enhancement displaced to lower altitudes (3-5 km) resulting from Asian CO, and attributes the lower tropospheric maximum to a combination of Asian and European influence (Figures 3 and 4). In fact European influence on CO was the highest calculated at CPO for spring 2001 (40 ppbv), however the simultaneous decrease in Asian contribution resulted in no overall increase in total modeled CO levels, consistent with observations. This European CO plume traveled below the Asian plume, and was initially exported over the Pacific behind the low pressure system ahead of the one which caused the dust storm. By April 13 the Asian plume, which is traveling at higher altitudes, has caught up with the European plume and both are arriving over North America at the same time.

**7.3. May 6 2001**

On May 6, the GEOS-CHEM model captures the observed CO and ozone enhancements between 1 and 3 km altitude (Figure 4 and 7). The CO enhancement is attributed to Asian

sources. For ozone, the model assigns the increase to a combination of a strong Asian component and a stratospheric contribution.

During the last days of April, the Siberian anticyclone extended to the East, over the Sea of Okhotsk, where it remained stationary for the first few days of May (Figure 13). As a cyclone approached this blocking high from the west on May 1, the strong pressure gradients between the two systems forced a northward surge of Asian pollution towards the Arctic. The Asian pollution traveled at low levels on the western and northern sides of the anticyclone. It then came under the influence of a developing surface low pressure system over Alaska and was rapidly transported along a northwesterly trajectory to the NE Pacific. The stratospheric intrusion was associated with the upper-level cut-off low and mixed in with the Asian pollution prior to its arrival over CPO. We confirmed the stratospheric origin of the air by examining TOMS total ozone satellite images, and by identifying dry air in water vapor GOES-West IR imagery and in the nearby Quillayute sounding.

Because the Asian anticyclone was the dominant pressure system guiding the export of Asian pollution, most of the transport initially remained at low levels. The northerly route (compared to the March 11 case) precluded strong photochemical loss of ozone, thus explaining the large 12-15 ppbv Asian ozone above CPO (Figure 7).

**8. Conclusions**

During the PHOBEA-II project, continuous observations of CO, ozone, and aerosols were obtained between March 9 and May 31, 2001 at the Cheeka Peak Observatory (48.3°N, 124.6°W, 480 m), a coastal site in Washington state. These observations were complemented by twelve vertical profiles (0-6 km) conducted above CPO with a twin-engine Beechcraft Duchess

aircraft. The PHOBEA-II project was conducted at the same time as the TRACE-P and ACE-Asia field missions, which sampled the western north Pacific troposphere. The GEOS-CHEM chemical transport model forecasts were successfully used not only to probe a number of trans-Pacific pollution transport episodes in the NE Pacific, but also to gather a representative dataset throughout the spring.

The GEOS-CHEM model provides an excellent simulation of CO observations both at the ground and aloft, reproducing average levels and day-to-day variability. The model's ability in capturing CO observations implies a good understanding of CO sources (in particular Asian sources), loss, and transport mechanisms.

For ozone, the model yields a good simulation of the aircraft profiles but systematically underestimates the ground-based observations by 11 ppbv. The poor correlation between observed and modeled ozone reflects the model overestimate of nearby North American influence on ozone because of the model's coarse horizontal resolution.

With GEOS-CHEM simulations tagging CO and ozone according to source regions, we examined the impact of Asian and European sources on the composition of the NE Pacific troposphere. We find that 33% of CO in the 0-6 km near CPO comes from Asian sources and 16% from European sources, while North American sources account for 13%. At the surface, North American CO sources become more important (17%) and account for 77% of the variability in CPO observations. In the 0-6 km column near CPO, direct transport of ozone produced over Asia and Europe respectively account for 12% and 5% of ozone. We estimate that the full contribution from Asian emissions to $O_3$ in the 0-6 km column (including secondary production of ozone from export of Asian PAN and $NO_x$ to the free troposphere) is at least 16%.

Based on back trajectories combined with observed layers of enhanced gases and aerosols, *Jaffe et al.* [2002] identified three episodes of long-range transport of air pollutants and dust from Asia. The GEOS-CHEM model captures two of these episodes, and confirms the Asian origin of these airmasses. Using the tagged CO simulation, we identified an additional strong long-range transport event in the surface observations and linked it to strong post-frontal boundary layer outflow observed in the western Pacific during TRACE-P [*Liu et al*., this issue; *Carmichael et al.*, this issue]. In all three cases reproduced by the model, both observations and model show clear enhancements in CO. However, only in one of these cases is ozone enhanced. This enhancement is captured by the model and is attributed to a combination of transport of Asian ozone at high latitudes and ozone of stratospheric origin. In the other two cases, the modeled contribution from Asian ozone increases to 8-10 ppbv but the total levels of ozone are not significantly enhanced, rendering detection of Asian influence on ozone difficult. Thus while detection of ozone enhancements and attribution to Asian long-range transport is a difficult task on the basis of observations alone, combining observations with a global model driven by assimilated meteorological observations allows a more quantitative understanding of the current impact of Asian emissions in the NE Pacific troposphere.

**Acknowledgments**. This work was supported by funding from the National Science Foundation (ATM-0089929) to UW-Bothell. Harvard acknowledges support from the NASA Atmospheric Chemistry Modeling and Analysis Program. Lyatt Jaeglé was supported in part by National Science Foundation ADVANCE Cooperative Agreement No. SBE-0123552. We would like to thank the pilots at Northway Aviation (Everett, WA) for their assistance during the PHOBEA-II experiment.

**References**

Akimoto, H. and H. Narita, Distribution of $SO_2$, $NO_x$, and $CO_2$ Emissions from Fuel Combustion and Industrial Activities in Asia with $1^o$x$1^o$ Resolution, *Atmos. Environ., 28*, 213-225, 1994.

Andreae, M. O., H. Berresheim, T. W. Andreae, M. A. Kritz, T. S. Bates, and J. T. Merrill, Vertical distribution of dimethylsulfide, sulfur dioxide, aerosol ions, and radon over the northeast Pacific Ocean, *J. Atmos. Chem., 6*, 149-173, 1988.

Berntsen, T.K., S. Karlsdottir, and D.A. Jaffe, Influence of Asian emissions on the composition of air reaching the North Western United States, *Geophys. Res. Lett.*, *26*, 2171-2174, 1999.

Bey, I., D.J. Jacob, R.M. Yantosca, J.A. Logan, B.D. Field, A. M. Fiore, Q. Li, H.Y. Liu, L.J. Mickley, and M.G. Schultz, Global modeling of tropospheric chemistry with assimilated meteorology: Model description and evaluation, *J. Geophys. Res*., *106*, 23,073-23,096, 2001a.

Bey, I., D.J. Jacob, J.A. Logan, and R.M. Yantosca, Asian chemical outflow to the Pacific: Origins, pathways and budgets, *J. Geophys. Res*., *106*, 23,097-23,114, 2001b.

Bey, I., et al., *J. Geophys. Res*., this issue, 2002.

Bognar, J. A., and J. W. Birks, Miniaturized ultraviolet ozonesonde for atmospheric measurements, *Analyt. Chem., 68*, 3059-3062, 1996.

Carmichael, G.R., I. Uno, M.J. Phadnis, Y. Zhang, and Y. Sunwoo, Tropospheric ozone production and transport in the springtime in east Asia, J. Geophys. Res., 103, 10,649-10,671, 1998.

Carmichael, G.R., and 20 others, Regional-Scale Chemical Transport Modeling in Support of Intensive Field Experiments: Overview and Analysis of the TRACE-P Observations, *J. Geophys. Res*., this issue, 2002.

Cooper, O.R., J.L. Moody, D.D. Parrish, M. Trainier, T.B. Ryerson, J.S. Holloway, G. Hubler, F.C. Fehsenfeld, and M.J. Evans, Trace gas composition of midlatitude cyclones over the western North Pacific: a conceptual model, *J. Geophys. Res*., *107*, 10.1029/2001JD000901, 2002.

Draxler, R.R., and G.D. Hess, Description of the Hysplit_4 modeling system, *NOAA Technical Memo ERL ARL-224*, 1997.

Duncan, B.N., J.A. Logan, I. Bey, R.V. Martin, D.J Jacob, and R.M. Yantosca, Model study of the variability and trends of carbon monoxide (1988-1997) 1. Model formulation, evaluation and sensitivity, submitted *to J. Geophys. Res*., 2002a.

Duncan, B.N., R.V. Martin, A.C. Staudt, R.M. Yevich, and J.A. Logan, Interannual and seasonal variability of biomass burning emissions constrained by remote-sensed observations, submitted *to J. Geophys. Res*., 2002b.

Elliott, S., D.R. Blake, R.A. Duce, C.A. Lai, I. McCreary, L.A. McNair, F.S. Rowland, A.G. Russell, G.E. Streit and R.P. Turco, Motorization of China implies changes in Pacific air chemistry and primary production, *Geophys. Res. Lett*., *24*, 2671-2674, 1997.

Fiore, A.M., et al., Background ozone over the United States in summer: Origin, trend and contributions to pollution episodes, *J. Geophys. Res*., *107 (D15)*, 10.1029/2001JD000982, 2002.

Fuelberg, H.E., C.M. Kiley, J.R. Hannan, D.J. Westberg, M.A. Avery, and R.E. Newell, Atmospheric transport during the Transport and Chemical Evolution Experiment over the Pacific (TRACE-P) experiment, *J. Geophys. Res*., this issue, 2002.

Gong, S.L., X.Y. Zhang, T.L. Zhao, I.G. McKendry, D.A. Jaffe, and N.M. Lu, Characterization of soil dust aerosol in China and its transport/distribution during 2001 ACE-Asia 2, Model simulation and validation, *J. Geophys. Res*., in press, 2002.

Heald, C.L., et al., Biomass burning emission inventory with daily resolution: application to aircraft observations of Asian outflow, *J. Geophys. Res*., this issue, 2002.

Hess, P. G., S. Flocke, J.-F. Lamarque, M.C. Barth, and S. Madronich, Episodic modeling of the chemical structure of the troposphere as revealed during the spring MLOPEX 2 intensive, *J. Geophys. Res*., *105*, 26,809-26,840, 2000.

Huebert, B., T. Bates, P. Russell, J. Seinfeld, M. Wang, M. Uematsu, and Y.J. Kim, An overview of ACE-Asia: Strategies for quantifying the relationships between Asian aerosols and their climatic impacts, submitted to *J. Geophys. Res*., 2002.

Husar, R.B., et al., The Asian dust events of April 1998, *J. Geophys. Res*., *106*, 18,317-18,333, 2001.

Jacob, D.J., J.A. Logan, and P.P. Murti, Effect of rising Asian emissions on surface ozone in the United States, *Geophys. Res. Lett.*, *26*, 2175-2178, 1999.

Jacob, D.J., J.H. Crawford, M.M. Kleb, V.E. Connors, R.J. Bendura, J.L. Raper, et al., The Transport and Chemical Evolution over the Pacific (TRACE-P) mission: Design, execution, and overview of results, *J. Geophys. Res*., this issue, 2002.

Jaffe, D.A., T. Anderson, D. Covert, R. Kotchenruther, B. Trost, J. Danielson, W. Simpson, T. Berntsen, S. Karlsdottir, D. Blake J. Harris, G. Carmichael, and I. Uno, Transport of Asian air pollution to North America, *Geophys. Res. Lett.*, *26*, 711-714, 1999.

Jaffe, D.A., T. Anderson, D. Covert, B. Trost, J. Danielson, W. Simpson, D. Blake, and J. Harris, Observations of ozone and related species in the northeast Pacific during the PHOBEA

campaigns: 1. Ground-based observations at Cheeka Peak, J. Geophys. Res., *106*, 7449-7461, 2001.

Jaffe, D., I. McKendry, T. Anderson, and H. Price, Six new episodes of trans-Pacific transport of air pollutants, *Atmos. Environ*., in press, 2002.

Kiley, C.M., H.E. Fuelberg, D. Allen, G.R. Carmichael, D.J. Jacob, C. Mari, P.I. Palmer, B. Pierce, K. Pickering, Y. Tang, O. Wild, T.D. Fairlie, J.A. Logan, and D.G. Streets, An intercomparison and validation of aircraft-derived and simulated CO from seven chemical transport models during the TRACE-P experiment, *J. Geophys. Res.,* this issue, 2002.

Kotchenruther, R.A., D.A. Jaffe, H.J. Beine, T.L. Anderson, J.W. Bottenheim, J.M. Harris, D.R. Blake, and R. Schmitt, Observations of ozone and related species in the northeast Pacific during the PHOBEA campaigns: 2. Airborne observations, *J. Geophys. Res*., *106*, 7463-7483, 2001a.

Kotchenruther, R., D.A. Jaffe, and L. Jaeglé, Ozone photochemistry and the role of PAN in the springtime northeastern Pacific troposphere: Results from the PHOBEA campaign, *J. Geophys. Res*., *106*, 28731-28743, 2001b.

Kritz, M.A., J.C. LeRoulley, and E.F. Danielsen, The China Clipper: Fast advective transport of radon-rich air form the Asian boundary layer to the upper troposphere near California, *Tellus*, *42B*, 46-61, 1990.

Lee, S.-H., H. Akimoto, H. Nakane, S. Kurnosenko, and Y. Kinjo, Lower tropospheric ozone trend observed in 1989-1997 at Okinawa, Japan, *Geophys. Res. Lett*., *25*, 1637-1640, 1998.

Li, Q., et al., Transatlantic transport of pollution and its effects on surface ozone in Europe and North America, *J. Geophys. Res*., 10.1029/2001JD001422, 2002a.

Li, Q., D.J. Jacob, T.D. Fairlie, H. Liu, R.M. Yantosca, and R.V. Martin, Stratospheric versus pollution influences on ozone at Bermuda: Reconciling past analyses*, J. Geophys. Res*., in press, 2002b.

Liu, H., D.J. Jacob, L.Y. Chan, S.J. Oltmans, I. Bey, R.M. Yantosca, J.M. Harris, B.N. Duncan, and R.V. Martin, Sources of tropospheric ozone along the Asian Pacific Rim: An analysis of ozonesonde observations*, J. Geophys. Res.,* in press, 2002.

Liu, H., D.J. Jacob, I. Bey, R.M. Yantosca, B.N. Duncan, and G.W. Sachse, Transport pathways for Asian combustion outflow over the Pacific: Interannual and seasonal variations, *J. Geophys. Res.,* this issue, 2002.

Logan, J.A, M.J. Prather, F.C Wofsy and M.B. McElroy, Tropospheric Chemistry: A Global Perspective, *J. Geophys. Res*., *86*, 7210-7254, 1981.

Logan, J.A., Trends in the vertical distribution of ozone: an analysis of ozone sonde data, *J. Geophys. Res*., *99*, 25553-25585, 1994.

Martin, R.V., D.J. Jacob, J.A. Logan, I. Bey, R.M. Yantosca, A.C. Staudt, Q. Li, A.M. Fiore, B.N. Duncan, H. Liu, P. Ginoux, and V. Thouret, Interpretation of TOMS observations of tropical tropospheric ozone with a global model and in-situ observations, *J. Geophys. Res.*, *107*(D18), 4351, 10.1029/2001JD001480, 2002.

Martin, R.V., D.J. Jacob, R.M. Yantosca, M. Chin, and P. Ginoux, Global and Regional Decreases in Tropospheric Oxidants from Photochemical Effects of Aerosols*, J. Geophys. Res.,* submitted, 2002.

Mauzerall, D. L., D. Narita, H. Akimoto, L. Horowitz, S. Walters, D. A. Hauglustaine, and G. Brasseur, Seasonal characteristics of tropospheric ozone production and mixing ratios over

East Asia: A global three-dimensional chemical transport model analysis, *J. Geophys. Res., 105*, 17,895-17,910, 2000.

McKendry, I. G., J. P. Hacker, R. Stull, Long-range transport of Asian dust to the Lower Fraser Valley, British Columbia, Canada, *J. Geophys. Res., 106*, 18,361-18,370, 2001.

Newell, R.E., and M.J. Evans, Seasonal changes in pollutant transport to the North Pacific: the relative importance of Asian and European sources, *Geophys. Res. Lett*., *27*, 2509-2512, 2000.

Palmer, P. I., D. J. Jacob, K. Chance, R. V. Martin, R. J. D, Spurr, T. P. Kurosu, I. Bey, R. Yantosca, A. Fiore, and Q. Li. Air mass factor formulation for spectroscopic measurements from satellites: application to formaldehyde retrievals from GOME*, J. Geophys. Res., 106*, 14,539-14,550, 2001.

Palmer, P.I., Inverting for Asian emissions of CO using aircraft observations during TRACE-P, *J. Geophys. Res.,* this issue, 2002.

Parrish, D. D., C. J. Hahn, E. J. Williams, R. B. Norton, F. C. Fehsenfeld, H. B. Singh, J. D.Shetter, B. W. Gandrud, and B. A. Ridley, Indications of photochemical histories of Pacific air masses from measurements of atmospheric trace species at Pt. Arena, California, *J. Geophys. Res., 97*, 15,883-15,901, 1992.

Prather, M.J., and D. Ehhalt, Chapter 4: Atmospheric Chemistry and Greenhouse Gases, *in Climate Change 2001: The Science of Climate Change*, Intergovernmental Panel on Climate Change, Cambridge University Press, 2001.

Price, H.U., D.A. Jaffe, P.V. Doskey, I. McKendry, and T.L. Anderson, Vertical profiles of ozone, aerosols, CO and NMHCs in the Northeast Pacific during the TRACE-P and ACE-Asia experiments, *J. Geophys. Res.,* this issue, 2002.

Raatz, W.E., An anticyclonic point of view on low-level tropospheric long-range transport, *Atmos. Env*., *23*, 2501-2504, 1989.

Schubert, S.D., R.B. Rood, and J. Pfaendtner, An assimilated data set for earth science applications, *Bull. Am. Meteorol. Soc.*, *74*, 2331-2342, 1993.

Snow, J.A, J.B. Dennison, D.A. Jaffe, H.U. Price, J.K. Vaughan, B. Lamb, Aircraft measurements of air quality in Puget Sound: Summer 2001, submitted to *Atmos. Env*., 2002**.**

Staudt, A. C., D. J. Jacob, J. A. Logan, D. Bachiochi, T. N. Krishnamurti, and G. W. Sachse, Continental sources, transoceanic transport, and interhemispheric exchange of carbon monoxide over the Pacific*, J. Geophys. Res., 106 ,* 32,571-32,590, 2001.

Stohl, A., and T. Trickl, A textbook example of long-range transport: Simultaneous observations of ozone maxima of stratospheric and North American origin in the free troposphere over Europe, *J. Geophys. Res., 104,* 30,445-30,472, 1999.

Stohl, A., A 1-year lagrangian climatology of airstreams in the Northern Hemisphere troposphere and lowermost stratosphere, *J. Geophys. Res*., *106*, 7263-7279, 2001.

Streets, D.G., and S.T. Waldhoff, Present and future emissions of air pollutants in China: $SO_2$, $NO_x$, and CO, *Atmos. Environ*., *34*, 363-374, 2000.

Streets, D.G., T.C. Bond, G.R. Carmichael, S.D. Fernandes, Q. Fu, D. He, Z. Klimont, S.M. Nelson, N.Y. Tsai, M.Q. Wang, J.-H. Woo, and K.F. Yarber, An inventory of gaseous and primary aerosol emissions in Asia in the year 2000, *J. Geophys. Res.,* this issue*,* 2002.

Thulasiraman, S., N. T. O'Neill, A. Royer, B. N. Holben, D. L. Westphal, and L. J. B. McArthur, Sunphotometric observations of the 2001 Asian dust storm over Canada and the U.S., *Geophys. Res. Lett., 10.1029/2001GL014188*, 2002.

van Aardenne, J.A., G.R. Carmichael, H. Levy, D. Streets, and L. Hordijk, Anthropogenic $NO_x$ emissions in Asia in the period 1990-2020, *Atmos. Environ.*, *33*, 633-646, 1999.

Wild, O., and H. Akimoto, Intercontinental transport of ozone and its precursors in a three-dimensional global CTM, *J. Geophys. Res.*, *106*, 27,729-27,744, 2001.

WMO, *Scientific Assessment of ozone depletion: 1998*, World Meteorological organization, Geneva, Switzerland, 1999.

Yevich, R, and J.A. Logan, An assessment of biofuel use and burning in agricultural waster in the developing world, *Global Biogeochem. Cycles*, submitted, 2002.

Yienger, J.J., M. Galanter, T.A. Holloway, M.J. Phadnis, S.K. Guttikunda, C.R. Carmichael, W.J. Moxim, and H. Levy II, The episodic nature of air pollution transport from Asia to North America, *J. Geophys. Res*., *105*, 26,931-26,945, 2000.

**Figure captions.**

**Figure 1.** April 10 2001 (0 GMT) GEOS-CHEM model forecast for April 13 2001 at 6 GMT. Total CO concentrations predicted at 600 hPa. The location of our measurement area at and above the Cheeka Peak Observatory (CPO: 48.3˚N, 124.6˚W) is indicated with an arrow.

**Figure 2.** Timeseries of column CO concentrations at CPO (below 6 km altitude) between March 9 and May 31, 2001. The grey circles represent the observations on the twelve flight days, where surface levels of CO are taken from the ground-based observations. The solid black line shows the hourly GEOS-CHEM column. Also shown are the individual anthropogenic contributions from Asia (black line and triangles), North America (grey line) and Europe (dashed line) from the tagged CO simulation. Note the factor of two difference in scale for the total CO columns (left axis) and individual tagged components (right axis).

**Figure 3.** Top panel**:** March 9-May 31 2001 comparison between hourly model (black line) and observations (grey line with circles) at CPO for CO. The GEOS-CHEM model is sampled at the location and altitude of CPO. Bottom panel: Timeseries of individual modeled contributions from Asian (solid line with triangles), North American (grey line), and European (dashed line) source regions at Cheeka Peak. The arrow indicates the March 11 long-range transport event discussed in section 7.

**Figure 4.** Profiles of CO observed during the 12 flights of the Duchess aircraft between March 29 and May 6 2001. The observations (grey circles connected by grey lines) are compared to results from the GEOS-CHEM model (black lines) sampled at the location of the observations within 24 hours of each flight. Individual contributions from Asian, North American, and European source regions are also shown. The grey square symbols indicate simultaneous observations of CO at the ground.

**Figure 5.** Scatter plot of daily averaged observed concentrations and modeled concentrations of CO and $O_3$ for the CPO ground site (panels a and c), and aircraft profiles (panels b and d) during spring 2001. The mean mixing ratios (±standard deviations) of the measured and modeled values are indicated in each panel, as well as the mean ratio between model and observations, and the correlation coefficient ($r^2$). A line with a 1:1 slope is indicated with a dashed line.

**Figure 6.** Top panel**:** March 9-May 31 2001 comparison between hourly model (black line) and observations (grey line with circles) at CPO for ozone. Bottom panel: Timeseries of individual modeled contributions from Asian, North American, and European source regions at Cheeka Peak from the tagged-$O_x$ simulation.

**Figure 7.** Ozone profiles during the 12 flights of the Duchess aircraft between March 29 and May 6 2001. The observations (grey circles connected by grey lines) are compared to results from the GEOS-CHEM model (black lines) sampled at the location of the observations within 24 hours of each flight. The grey square symbols indicate simultaneous observations of CO at the ground. Individual contributions from Asian, North American, European, and stratospheric source regions from the tagged-$O_x$ simulation are also shown. Note that the individual contributions have been scaled by a factor of two for clarity.

**Figure 8.** Modeled mean concentrations (0-6 km altitude) of North American, Asian and European anthropogenic CO and ozone for March 9-May 31 2001. The arrows represent the tracer horizontal mass fluxes between 0 and 6 km altitude.

**Figure 9.** March 9-May 31 2001 vertical cross section at 125 W° of tagged CO and ozone fluxes (shaded contours in ppbv) from North American, Asian and European anthropogenic sources. The dashed contour lines (in units of $10^{-10}$ moles $s^{-1}$ $cm^{-2}$) represent horizontal fluxes of the tracers. Positive values are for westerly fluxes, while negative fluxes (hatched areas) represent easterly fluxes.

**Figure 10.** March 9-May 31 2001 mean concentrations (0-6 km altitude) and vertical cross section at 125 W° of *Delta* $O_3$ (=standard simulation-simulation without Asian emissions).

**Figure 11.** Time height cross section of Asian and European contributions to CO (in ppbv) at CPO. The vertical lines show the timing and vertical extent of PHOBEA-II flights.

**Figure 12**. Top panels: Daily Asian CO mixing ratios (in ppbv, colored contours) averaged between 0 and 6 km for March 4, March 8 and March 11 2001. The arrows show averaged horizontal fluxes. Bottom panels: Sea level pressure for March 4, March 8 and March 11 2001.

**Figure 13.** Top panels: Daily Asian CO mixing ratios (in ppbv, colored contours) at 2.5 km (740 hPa) for May 1, 3 and 5 2001. The arrows show averaged horizontal fluxes. Bottom panels: Sea level pressure for May 1, 3 and 5 2001.

**Table 1.** Source contributions to CO over the Northeastern Pacific from the tagged CO simulation[a]

| Source Regions[b] | Northeastern Pacific: 0-6 km columns 35-60˚N, 165˚W-125˚W | Cheeka Peak Observatory: 0-6 km columns 38.3˚N, 124.8˚W | Cheeka Peak Observatory: 38.3˚N, 124.8˚W, 480 m |
|---|---|---|---|
| Fuel combustion[c] | | | |
| North America | 1.8[a] (10.7%) | 2.2[a] ( 12.9%) | 25[e] ( 17%) |
| Europe | 2.7 (16.1%) | 2.7 ( 15.8%) | 25 ( 17%) |
| Asia | 4.6 (27.4%) | 4.5 ( 26.8%) | 36 ( 25%) |
| Others | 0.2 ( 1.4%) | 0.2 ( 1.4%) | 2 ( 2%) |
| Biomass burning | | | |
| Asia | 1.1 ( 6.7%) | 1.0 ( 5.9%) | 6.9 ( 4.8%) |
| Others | 1.3 ( 8.1%) | 1.3 ( 7.8%) | 9.1 ( 6.2%) |
| Atmospheric Production[d] | 4.9 (29.6%) | 4.9 (29.4%) | 41 (28%) |
| Total | 16.6 (100%) | 16.8 (100%) | 145 (100%) |

[a]Values are mean tropospheric columns (in $10^{17}$ molecules/cm$^2$) below 6 km altitude for March 9-May 31, 2001 from the tagged-CO simulation. Percentages are indicated in parenthesis.

[b]Source regions are defined as follows: North America (24-88˚N;142.5-47.5˚W), Europe (36-88˚N; 17.5˚W-65˚E), Asia (-12.5-88˚N; 65-153˚E).

[c]Fuel combustion includes fossil fuel and biofuel combustion.

[d]Atmospheric Production includes CO production from the oxidation of methane, isoprene, monoterpenes, acetone, and methanol.

[e]In this last column, values are in mixing ratios (in ppbv) for the tagged-CO simulation sampled at the location of CPO for March 9-May 31, 2001 (Figure 3).

**Table 2.** Chemical contributions to odd-oxygen ($O_x$) over the Northeastern Pacific from the tagged $O_x$ simulation

| Source Regions[a] | Northeastern Pacific: 0-6 km column 35-60˚N, 165˚W-125˚W | Cheeka Peak Observatory: 0-6 km column 38.3˚N,124.8˚W | Cheeka Peak Observatory: Mixing ratios 38.3˚N,124.8˚W,480 m |
|---|---|---|---|
| Lower troposphere | | | |
| North America | 3.7[b] (6.5%) | 5.2[b] (9.0%) | 7.0[c] (18%) |
| Europe | 2.9 (5.1%) | 2.8 (4.8%) | 2.2 (6%) |
| Asia | 7.3 (12.8%) | 6.9 (12.1%) | 4.2 (11%) |
| Pacific | 6.6 (11.6%) | 6.7 (11.6%) | 6.6 (17%) |
| Others | 4.7 (8%) | 4.2 (7.6%) | 2.6 (7%) |
| Middle troposphere | 13.8 (24.1%) | 13.5 (23.5%) | 6.3 (16%) |
| Upper troposphere | 8.2 (14.4%) | 7.9 (13.9%) | 4.1 (11%) |
| Stratosphere | 10 (17.5%) | 10 (17.5%) | 5.5 (14%) |
| Total | 57.2 (100%) | 57.2 (100%) | 38.5 (100%) |

[a]Source regions are defined as: lower troposphere (700 hPa-surface), middle troposphere (700-400 hPa) and upper troposphere (400 hPa-tropopause). Subdivisions within the lower troposphere follow the same continental geographic regions which are defined in Table 1.

[b]Values are mean tropospheric columns (in $10^{16}$ molecules/cm$^2$) below 6 km altitude for March 9-May 31, 2001 from the tagged-$O_x$ simulation. Percentages are indicated in parenthesis.

[c]In this last column, values are in mixing ratios (in ppbv) for the tagged-$O_x$ simulation sampled at the location of CPO for March 9-May 31, 2001 (Figure 6).

**Table 3.** $O_x$ budget over the Northeastern Pacific[a]

| | Budget | | |
|---|---|---|---|
| | 0-3 km | 3-6 km | 6-12 km |
| Chemistry | | | |
| Production | 1.72 | 1.42 | 1.03 |
| Loss | -2.02 | -2.07 | -0.77 |
| Advection | | | |
| West | 5.41 | 19.8 | 45.3 |
| East | -4.46 | -16.5 | -38.1 |
| North | -1.17 | -2.46 | -3.34 |
| South | -1.19 | -1.04 | -4.05 |
| Vertical transport | | | |
| Top | 1.84 | 2.54 | 3.28 |
| Bottom | 0.0 | -1.84 | -2.54 |
| Deposition | | | |
| Wet | -0.49 | -0.12 | -0.02 |
| Dry | -0.67 | 0.0 | 0.0 |
| Net | -1.03 | -0.28 | 0.71 |

[a]Results are from the full chemistry simulation. Values are in Gmoles/day for March 9-May 31, 2001 averaged over the NE Pacific (35-60˚N, 165˚W-125˚W). Positive values correspond to net sources for that region.

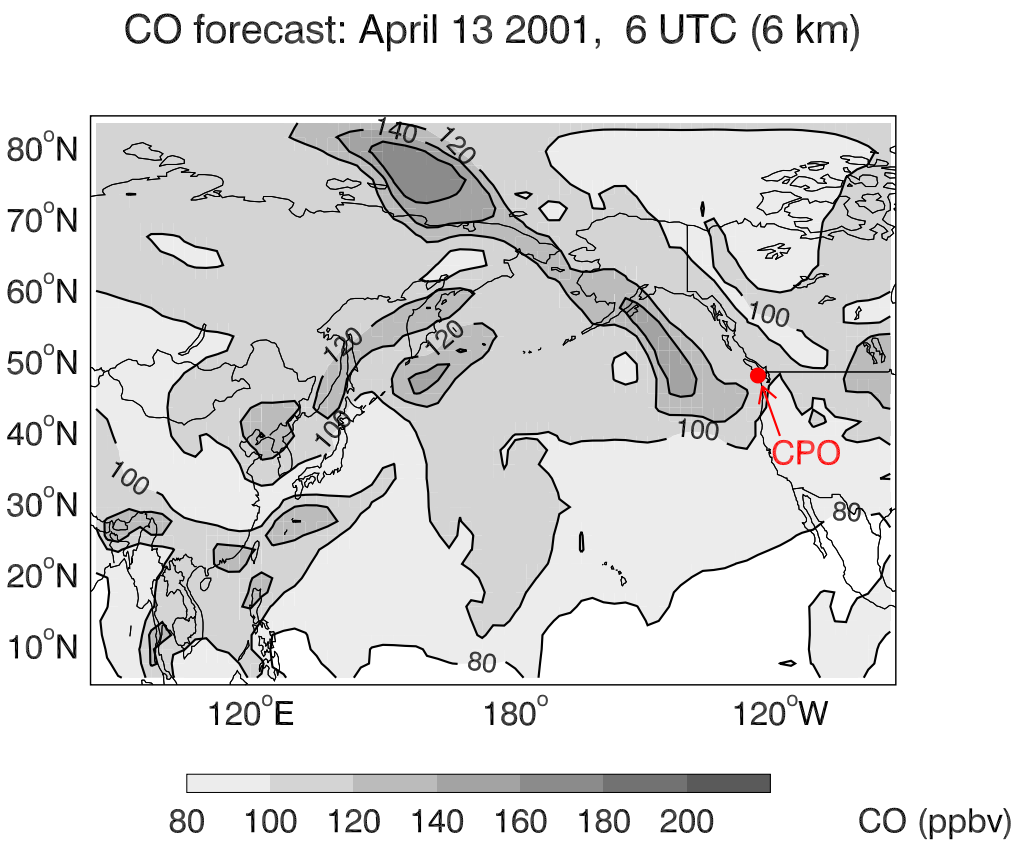


**Figure 1.** April 10 2001 (0 GMT) GEOS-CHEM model forecast for April 13 2001 at 6 GMT. Total CO concentrations predicted at 600 hPa. The location of our measurement area at and above the Cheeka Peak Observatory (CPO: 48.3˚N, 124.6˚W) is indicated with an arrow.

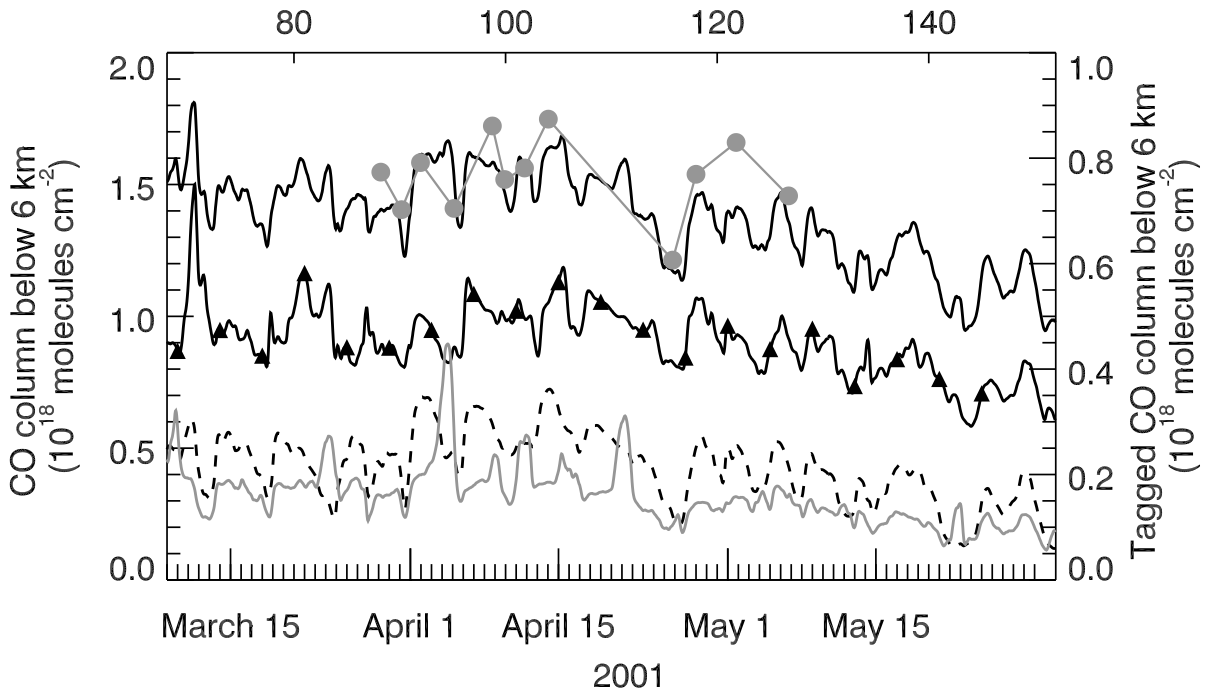


**Figure 2.** Timeseries of column CO concentrations at CPO (below 6 km altitude) between March 9 and May 31, 2001. The grey circles represent the observations on the twelve flight days, where surface levels of CO are taken from the ground-based observations. The solid black line shows the hourly GEOS-CHEM column. Also shown are the individual anthropogenic contributions from Asia (black line and triangles), North America (grey line) and Europe (dashed line) from the tagged CO simulation. Note the factor of two difference in scale for the total CO columns (left axis) and individual tagged components (right axis).

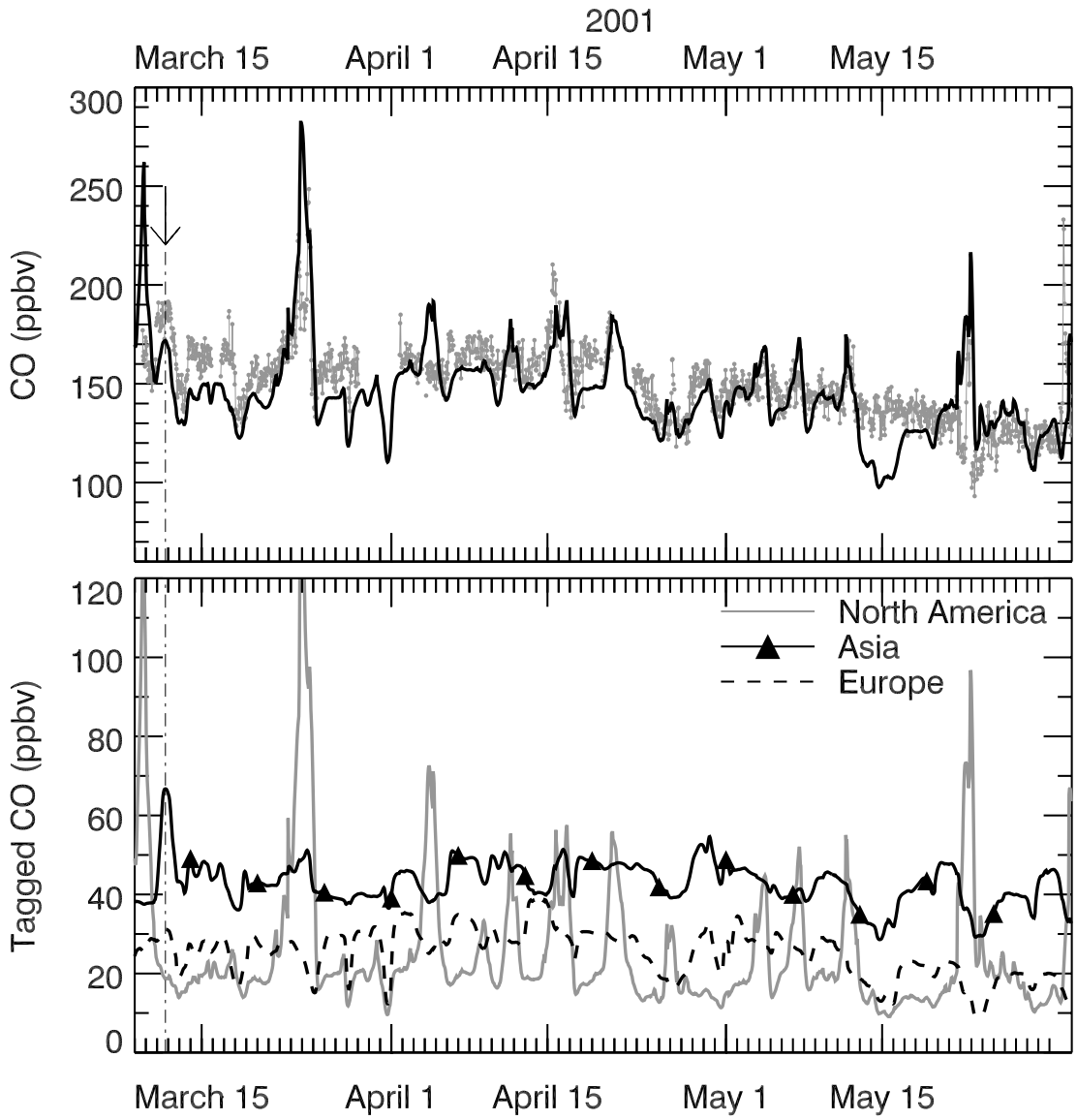


**Figure 3.** Top panel**:** March 9-May 31 2001 comparison between hourly model (black line) and observations (grey line with circles) at CPO for CO. The GEOS-CHEM model is sampled at the location and altitude of CPO. Bottom panel: Timeseries of individual modeled contributions from Asian (solid line with triangles), North American (grey line), and European (dashed line) source regions at Cheeka Peak. The arrow indicates the March 11 long-range transport event discussed in section 7.

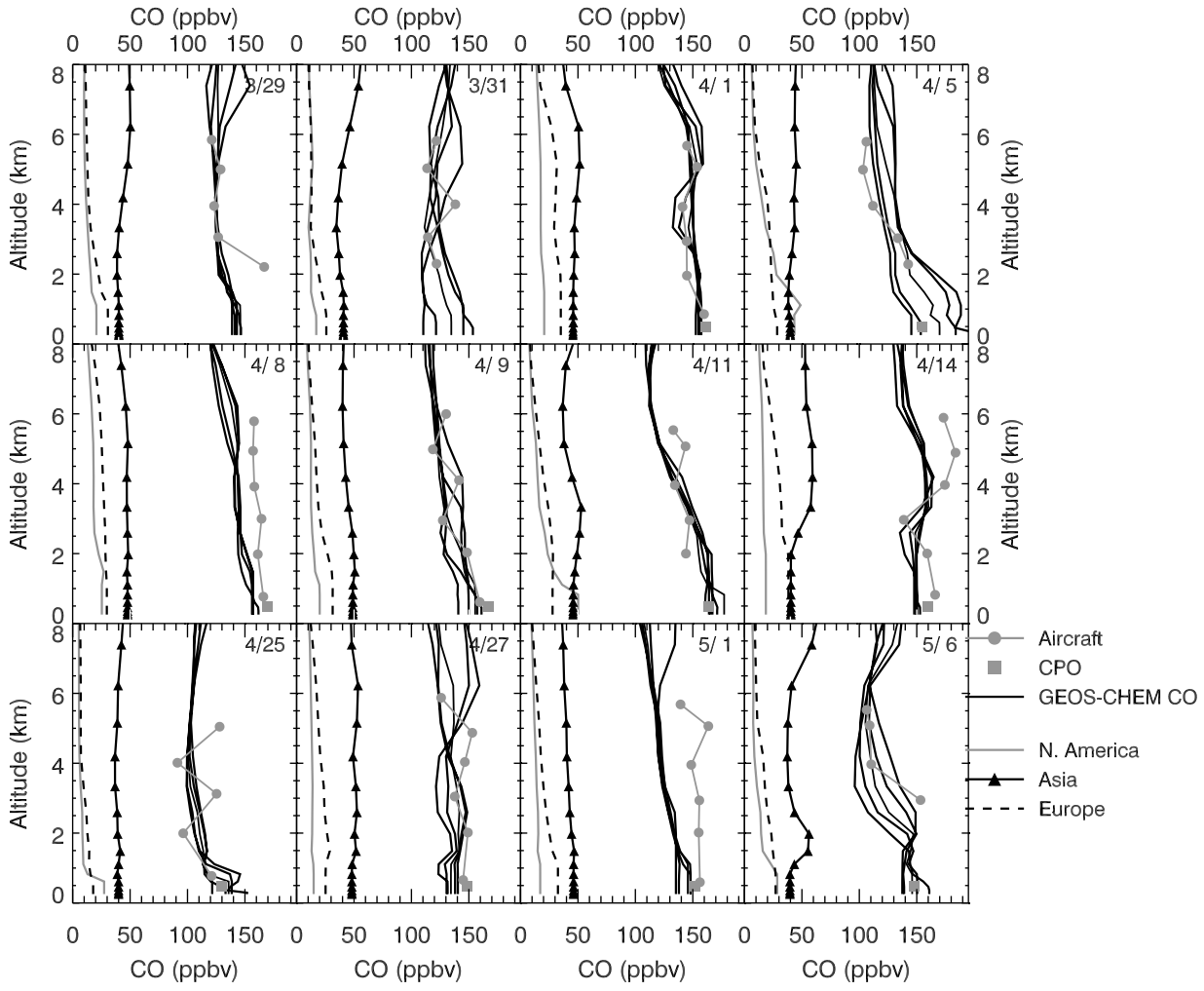


**Figure 4.** Profiles of CO observed during the 12 flights of the Duchess aircraft between March 29 and May 6 2001. The observations (grey circles connected by grey lines) are compared to results from the GEOS-CHEM model (black lines) sampled at the location of the observations within 24 hours of each flight. Individual contributions from Asian, North American, and European source regions are also shown. The grey square symbols indicate simultaneous observations of CO at the ground.

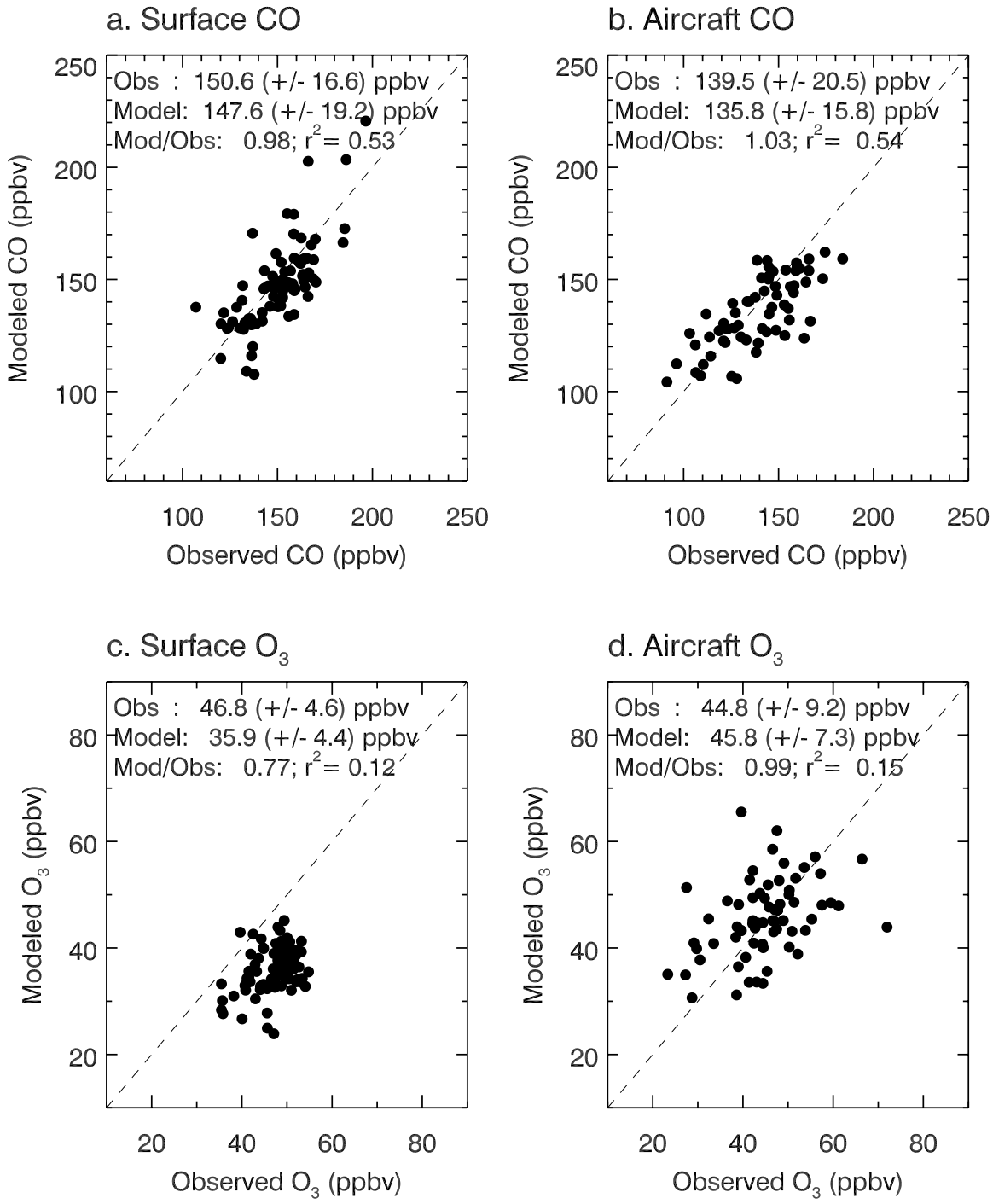


**Figure 5.** Scatter plot of daily averaged observed concentrations and modeled concentrations of CO and $O_3$ for the CPO ground site (panels a and c), and aircraft profiles (panels b and d) during spring 2001. The mean mixing ratios (±standard deviations) of the measured and modeled values are indicated in each panel, as well as the mean ratio between model and observations, and the correlation coefficient ($r^2$). A line with a 1:1 slope is indicated with a dashed line.

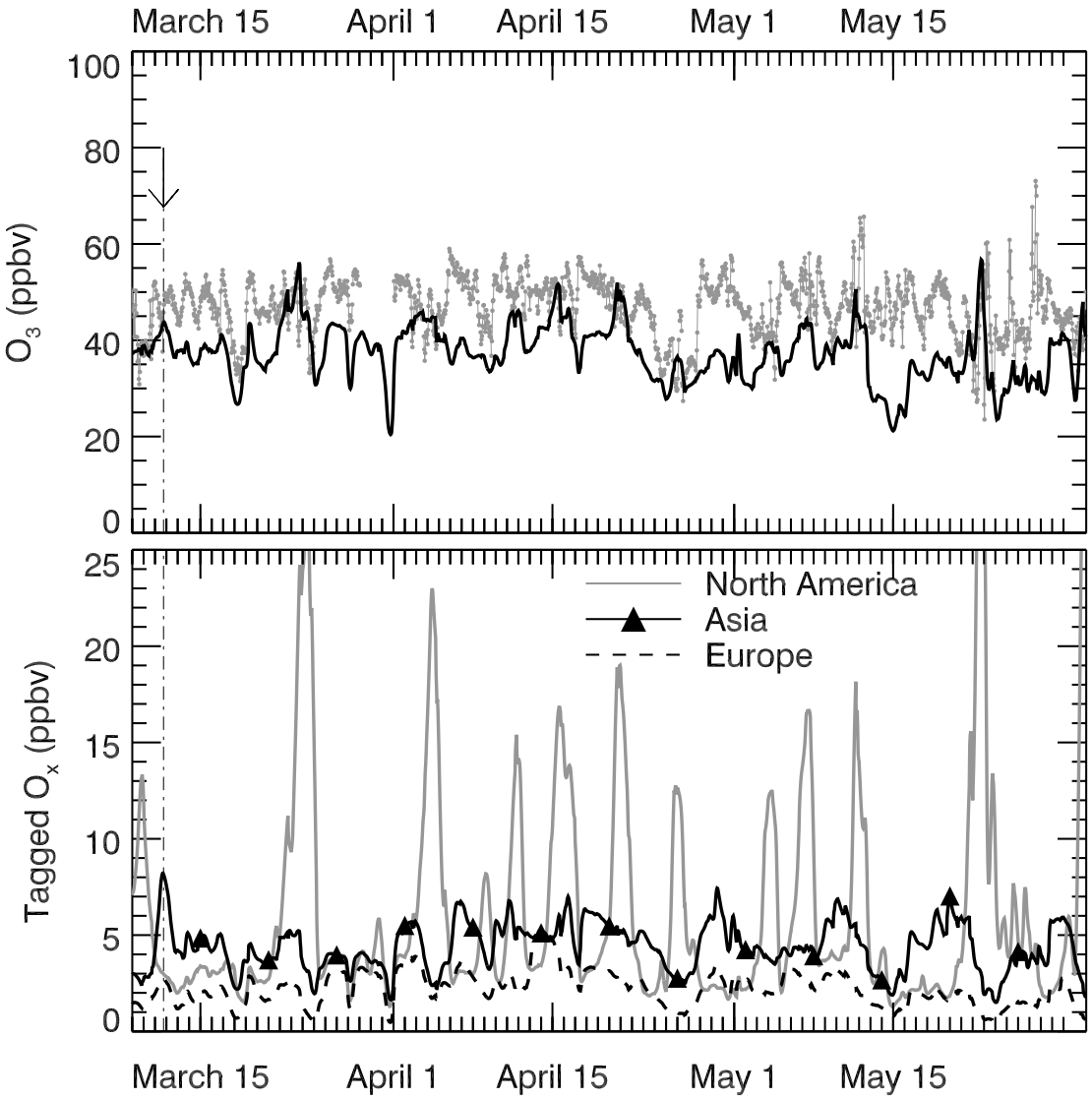


**Figure 6.** Top panel**:** March 9-May 31 2001 comparison between hourly model (black line) and observations (grey line with circles) at CPO for ozone. Bottom panel: Timeseries of individual modeled contributions from Asian, North American, and European source regions at Cheeka Peak from the tagged-$O_x$ simulation.

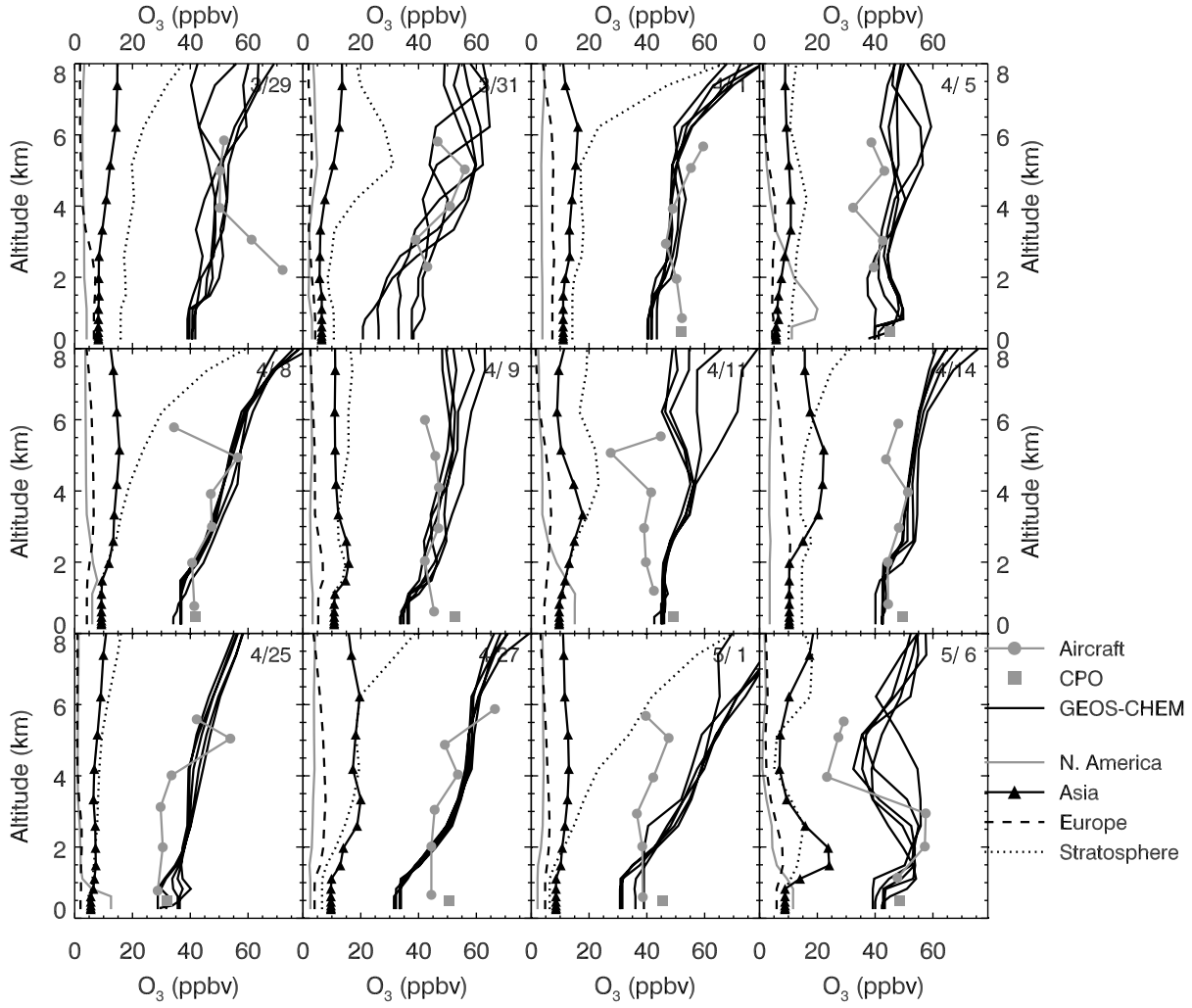


**Figure 7.** Ozone profiles during the 12 flights of the Duchess aircraft between March 29 and May 6 2001. The observations (grey circles connected by grey lines) are compared to results from the GEOS-CHEM model (black lines) sampled at the location of the observations within 24 hours of each flight. The grey square symbols indicate simultaneous observations of CO at the ground. Individual contributions from Asian, North American, European, and stratospheric source regions from the tagged-$O_x$ simulation are also shown. Note that the individual contributions have been scaled by a factor of two for clarity.

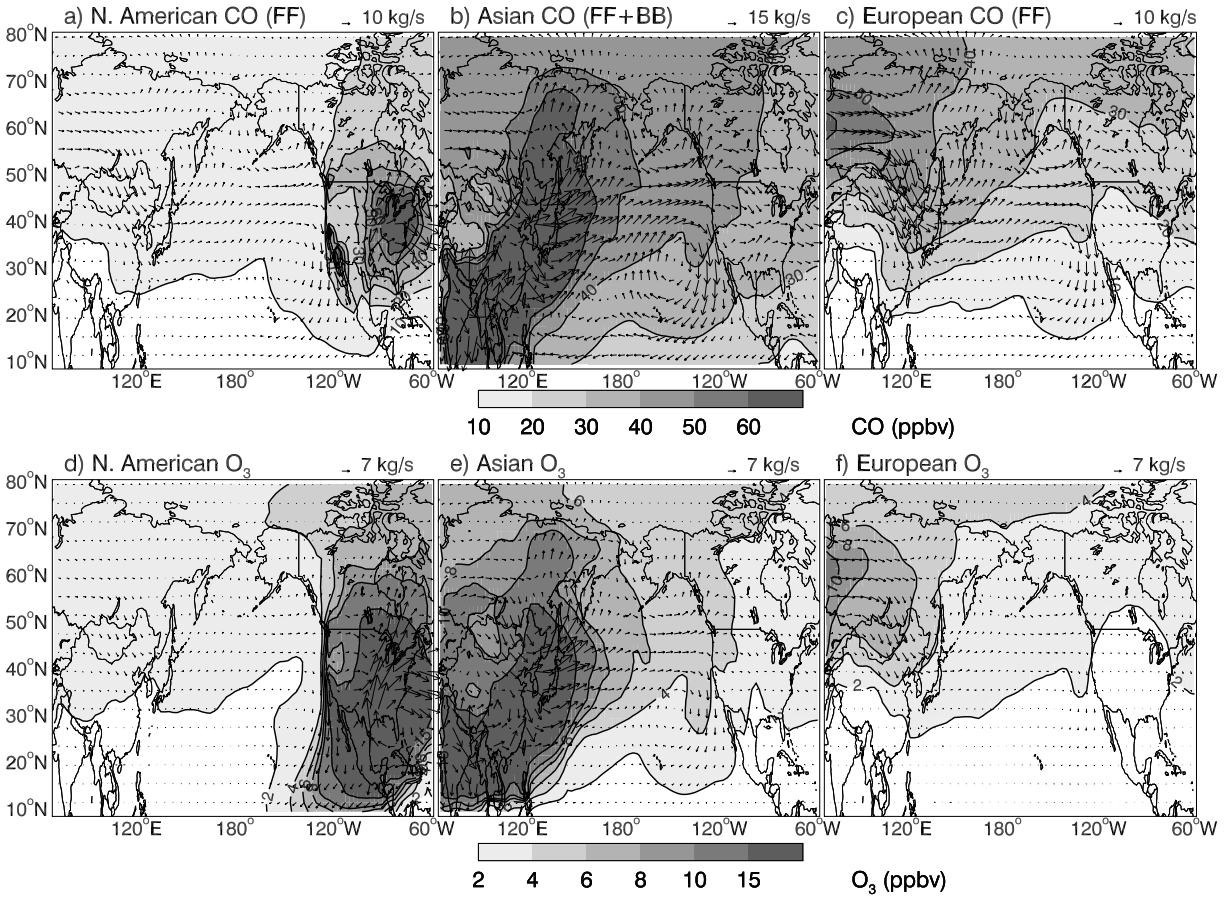


**Figure 8.** Modeled mean concentrations (0-6 km altitude) of North American, Asian and European anthropogenic CO and ozone for March 9-May 31 2001. The arrows represent the tracer horizontal mass fluxes between 0 and 6 km altitude.

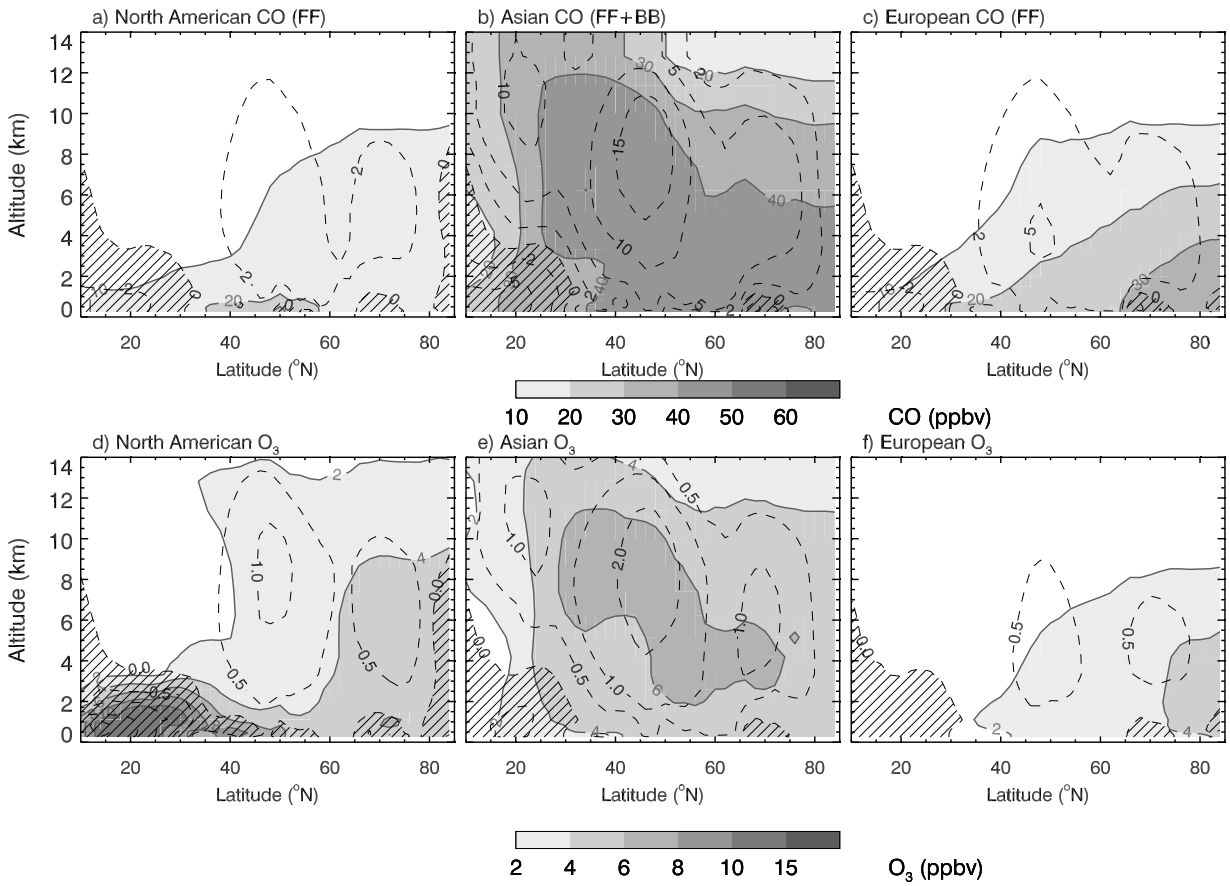


**Figure 9.** March 9-May 31 2001 vertical cross section at 125 W° of tagged CO and ozone fluxes (shaded contours in ppbv) from North American, Asian and European anthropogenic sources. The dashed contour lines (in units of $10^{-10}$ moles $s^{-1}$ $cm^{-2}$) represent horizontal fluxes of the tracers. Positive values are for westerly fluxes, while negative fluxes (hatched areas) represent easterly fluxes.

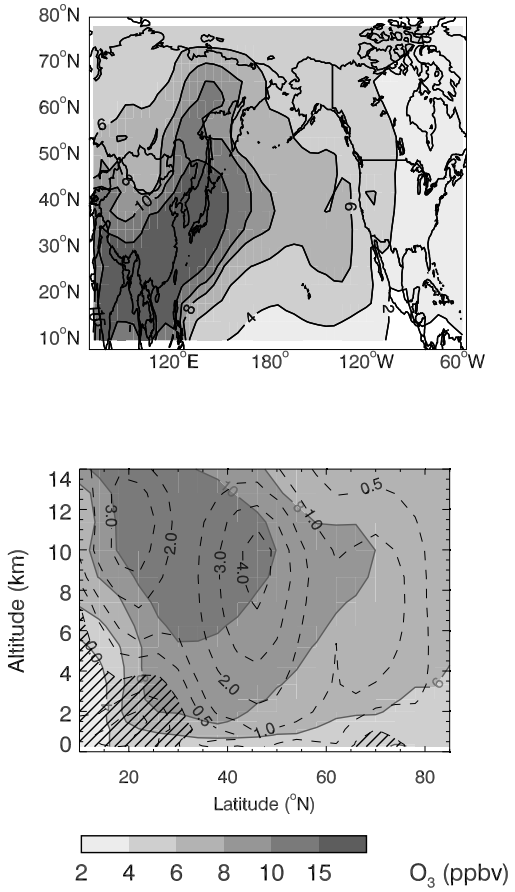


**Figure 10.** March 9-May 31 2001 mean concentrations (0-6 km altitude) and vertical cross section at 125 W° of *Delta $O_3$* (=standard simulation-simulation without Asian emissions).

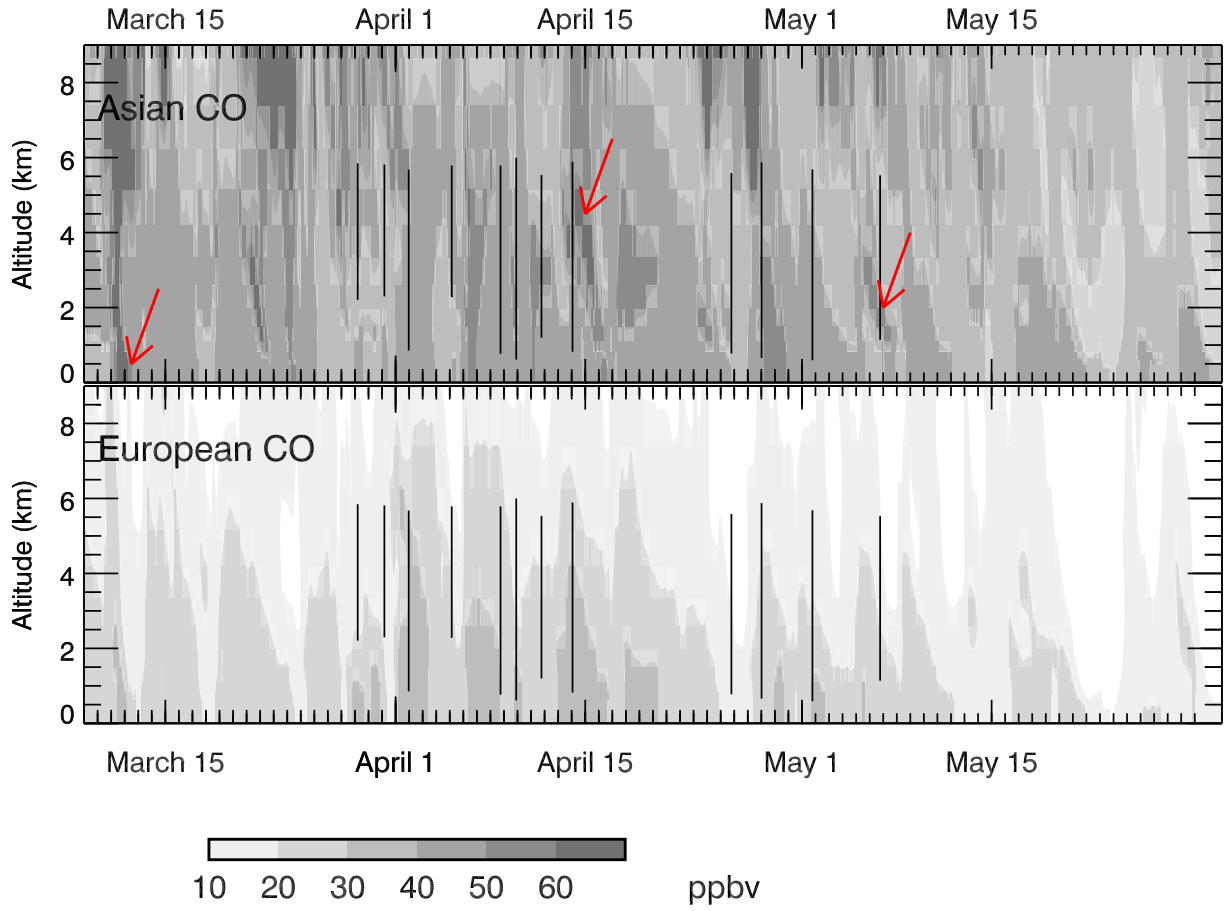


**Figure 11.** Time height cross section of Asian and European contributions to CO (in ppbv) at CPO. The vertical lines show the timing and vertical extent of PHOBEA-II flights. The arrows indicate the three long-range transport events discussed in section 7 (March 11; April 14; and May 6, 2001)

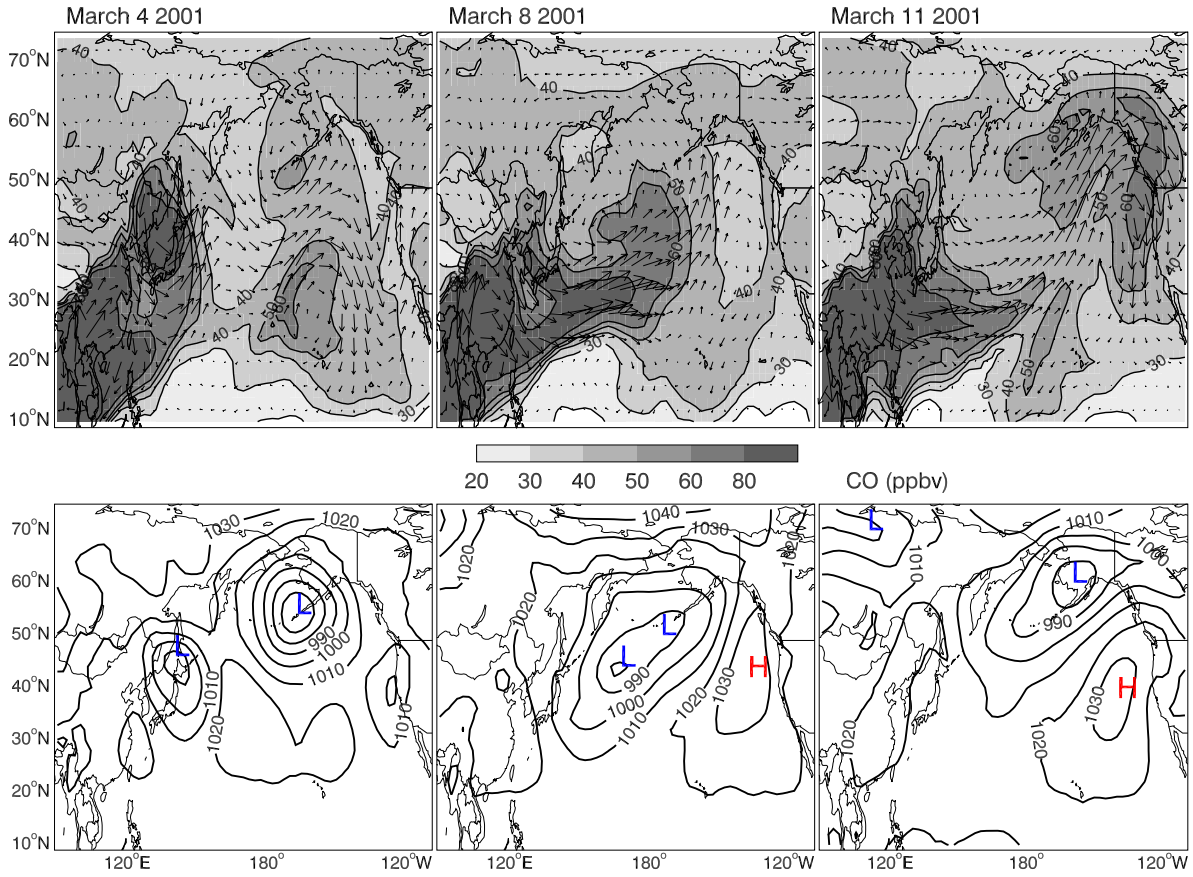


**Figure 12**. Top panels: Daily Asian CO mixing ratios (in ppbv, colored contours) averaged between 0 and 6 km for March 4, March 8 and March 11 2001. The arrows show averaged horizontal fluxes. Bottom panels: Sea level pressure for March 4, March 8 and March 11 2001.

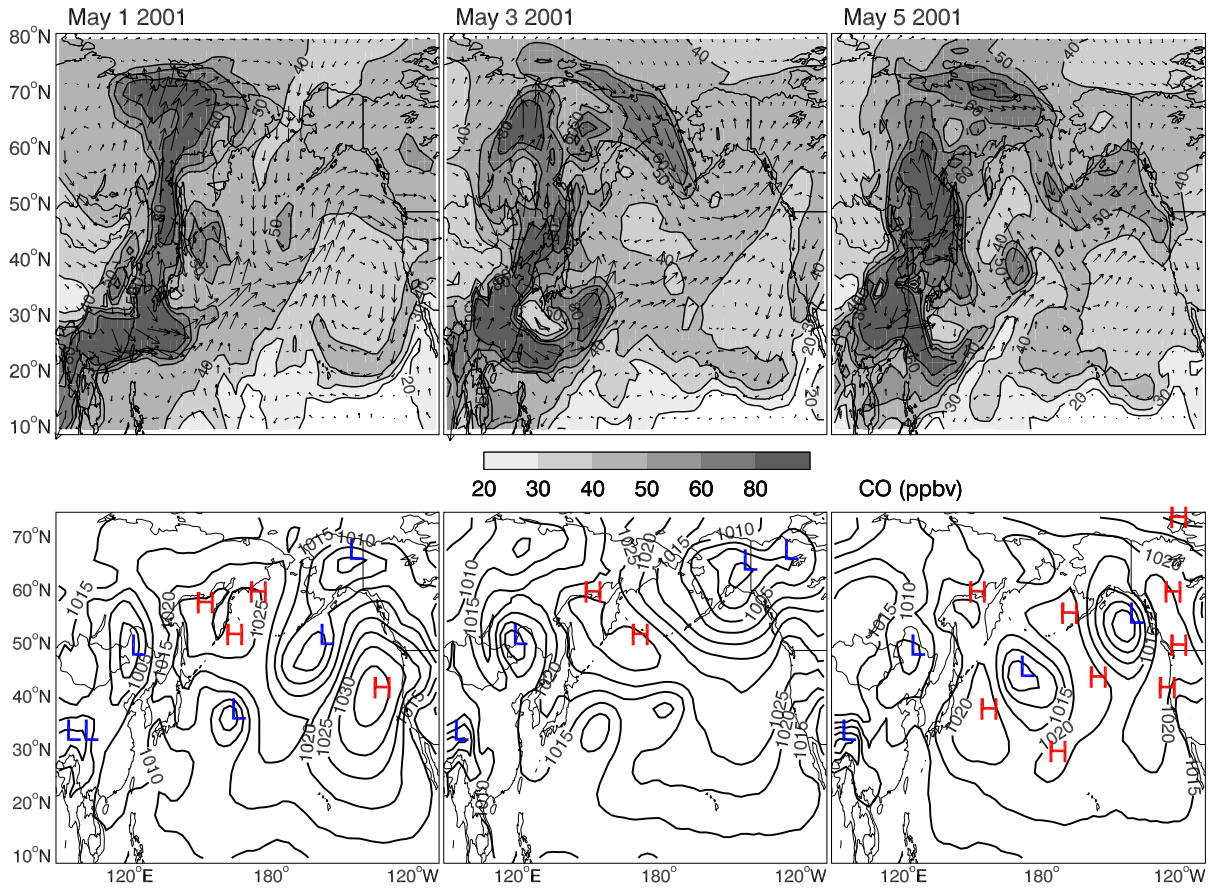


**Figure 13.** Top panels: Daily Asian CO mixing ratios (in ppbv, colored contours) at 2.5 km (740 hPa) for May 1, 3 and 5 2001. The arrows show averaged horizontal fluxes. Bottom panels: Sea level pressure for May 1, 3 and 5 2001.